MECHANICAL PROPERTIES OF SWOLLEN POLY(METHACRYLIC ACID)-*l*-POLYISOBUTYLENE CONETWORKS

Diploma Thesis
Master of Science in Material Science

EDWIN STEVEN REYES JACOME

Supervisors:

Prof. Béla Iván
Department of Organic Chemistry, Institute of Chemistry, ELTE TTK
and Polymer Chemistry and Physics Research Group,
Institute of Materials and Environmental Chemistry,
HUN-REN Research Centre for Natural Sciences

Dr. Szabolcs Pásztor
Polymer Chemistry and Physics Research Group,
Institute of Materials and Environmental Chemistry,
HUN-REN Research Centre for Natural Sciences

Dr. Ákos Szabó
Polymer Chemistry and Physics Research Group,
Institute of Materials and Environmental Chemistry,
HUN-REN Research Centre for Natural Sciences

Eötvös Loránd University, Faculty of Science
Budapest
2023

Acknowledgement

I would like to express my deepest gratitude to Professor Béla Iván for his guidance, unwavering support, and insightful supervision throughout the development of this thesis. His expertise, encouragement, and dedication have been instrumental in shaping this work and broadening my understanding of polymers.

I am also indebted to Dr. Szabolcs Pásztor and Dr. Ákos Szabó for their indispensable assistance and contributions. Their expertise, valuable insights, and willingness to share their knowledge have significantly enriched the research process and the quality of my work. Furthermore, I extend my appreciation to the members of the Polymer Chemistry and Physics Research Group of the Institute of Materials and Environmental Chemistry, HUN-REN Research Centre for Natural Sciences (Budapest, Hungary) for their support and encouragement during this academic journey.

I am profoundly grateful for the patience, encouragement, and support of my family, friends Bryan and Valeria, whose unwavering belief in me has been a constant source of inspiration.

Lastly, I want to express my heartfelt gratitude to my partner, Elizabeth. Her unwavering love, understanding, and encouragement have been the pillars that sustained me throughout this endeavor. Her support has been invaluable, and I am forever grateful.

Table of contents

I. Introduction

At school, children are taught that the pre-history of humanity is divided into four ages: Stone Age, Copper Age, Bronze Age, and Iron Age. The ages owe their names to the four materials that were the precursors of humanity's development. During the 20th and 21st centuries, the material that impacted human life the most was plastic. That's why researchers we are currently living in the Polymer Age, or as it appears in the media and popular science and technology news, the Age of Plastics [1].

According to the new by BBC, based on industrial reports, polymer (plastic) production soared from 2 million tons in 1950 to more than 400 million tons in 2020 [2]. Currently, the quality of life of humanity is closely related to the production of polymers. Today, it is not possible to imagine a life without these materials. Among the great variety of polymers currently available, the present work will focus its study on a special type of polymers, the so called amphiphilic conetworks (APCNs), which are composed of covalently linked, otherwise immiscible hydrophilic and hydrophobic polymer chains.

The first literatures regarding APCNs were published by Stadler [3] and Kennedy et al. [4] in 1988, basing their investigation on conetworks consisting of poly(ethylene oxide) and and polybutadiene, and methacryloyl-capped polyisobutylene and 2-dimethylaminoethyl methacrylate, respectively. One of the most update and accurate definition of these materials was provided by Erdodi and Kennedy [5,13]:

> *"Amphiphilic conetworks are two-component networks of covalently interconnected hydrophilic/hydrophobic (HI/HO) phases of cocontinuous morphology; as such they swell both in water and hydrocarbons and respond to changes in the medium by morphological isomerisation ('smart' networks)."*

Currently, the most widespread industrial application of APCNs is the formation of silicone hydrogels for manufacturing contact lenses. This application is very stable worldwide and millions of people are using it. Although contact lens manufacturing is the largest representative of APCNs, important advances have been made in recent decades in applications as diverse as drug delivery [6], tissue engineering [7] and matrices for heterogeneous enzyme catalysis [8].

Taking into consideration the possible applications of APCN, one of the most important challenges for its fruitful implementation in various applications is its resistance to different pHs. The human body exhibits a wide range of pH levels across various tissues, fluids, and compartments, each playing a vital role in physiological functions. Understanding and accommodating these different pH environments is crucial for biomaterials used in biomedicine to ensure their compatibility and effectiveness within the diverse systems of the body [9].

The present work analyzes the physical and swelling properties of poly(methacrylic acid)-*l*-polyisobutylene (PMAA-*l*-PIB, *l* = “linked by”) amphiphilic polymer conetworks through three different environments, basic, neutral, and acidic in the presence of a relatively high concentration of potassium chloride (0.05 M) in order to keep the ionic strength constant during all the measurements.

II. Literature overview and background

II.1. Amphiphilic polymer conetworks

Polymer gels are defined as three-dimensional networks, which are insoluble but able to swell by appropriate solvents. It’s important to note that the crosslinked polymer matrix never reaches an infinite dilution. The resulting gels, obtained by swelling polymer networks, are wet and soft, and unlike solid materials, these can undergo large deformation. Most of mammalian tissues are highly aqueous gel materials formed by proteins, polysaccharides and water [10]. There are multiple ways to classify gels including by the constituent polymers and by the crosslinkage, but the most common and used one is by its swelling material.

Considering that the polymer networks works as a host for a fluid that fill the interstitial space of the network, the fluid can be liquid (hydrogel, organogel, liogel, alcogel), gas (xerogel, aerogel) and solid (polymer – gel polymer, gel-gum) [11]. The most widely used polymer gels worldwide are hydrogels, which swell in water, however, in recent years, due to its attractive swelling properties in both hydrophilic and hydrophobic solvents, amphiphilic conetworks (APCNs) have drawn worldwide attention.

A simplified definition presented by Erdodi and Kennedy [5,13], defines APCNs as hydrogels which also swell in hydrocarbons. The main characteristic of these materials is the presence of hydrophilic and hydrophobic polymer chains in the polymer matrix, linked by covalent bonds.

The main difference between conetworks and copolymer networks is found in the continuity of the phases. The copolymer networks present randomly dispersed hydrophilic and hydrophobic monomeric units, but the polymer as macroscopic object does not present amphiphilic characteristics. In the amphiphilic conetworks, the HI/HO phases are arranged into separate phases rather than being randomly dispersed [12].

In the middle of Figure 1, it is presented how APCNs appear in the dry state [13]. In the presence of a common solvent, both phases swell, however, when exposed to a hydrophilic or hydrophobic solvent, only the soluble phase will swell while the insoluble phase will collapse trying to precipitate and separate from its counterpart.

Nonetheless, due to the covalent bonds present, the APCNs will maintain its continuity.

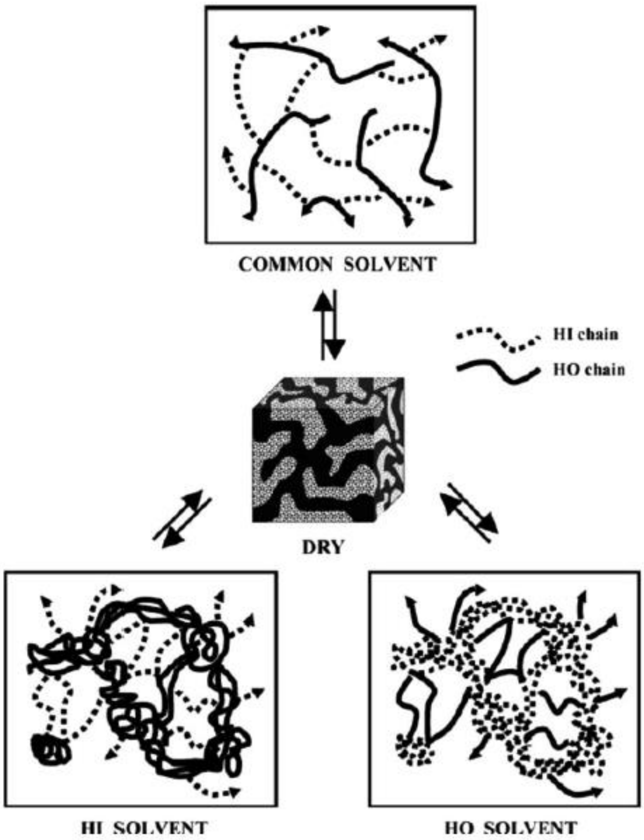

Figure 1. The effect of solvents on morphology of APCNs (taken from Ref. 13).

The presence of hydrophobic segments in APCNs provides an increase in the toughening of the polymer compared to a hydrogel formed only with hydrophilic segments. The increase in toughening is related to the reduction in the equilibrium aqueous degree of swelling, which compacts the material and provides certain degree of rigidity [14].

Due to the extensive and growing development of APCNs, various synthesis routes have been developed for their formation. Among the most relevant, we can find the following three major methods as described by Erdodi and Kennedy [13].

A) The random free radical copolymerization of monomers technique uses telechelic macromonomers as crosslinkers and small monomers as starting materials, and regarding how the radical is formed this process can be subdivided into thermally or photolytically initiated methods. Thermal initiation uses azo or peroxy initiators to create the starting radicals and can use hydrophilic or hydrophobic comonomers, always using a crosslinker of opposite nature and a good solvent for both monomers and crosslinker to complete the production APCNs [4,8,24-27]. This technique is well known and widely used due to its simplicity. Photoinitiation uses amphiphilic block copolymers and hydrophilic segments with vinyl carbonate end groups to facilitate the photo-crosslinking [8]. Contact lens manufacturers extensively employ this technique, which serves as the primary method for synthesizing the majority of commercially available APCNs.

B) Ionic sequential living polymerizations are characterized by its precision and ability to produce polymers with well-defined structures. In this technique, amphiphilic block copolymers are synthesized and the crosslinker is added at the end [5].

C) The chemical combination of hydrophilic and hydrophobic prepolymers technique involves the synthesis of APCNs by blending or chemically bonding together components that exhibit hydrophilic and hydrophobic properties. By carefully combining these pre-existing polymers or polymer precursors, it is possible to create new materials with amphiphilic character. For this method, only those hydrophilic and hydrophobic functionalized polymers can be applied which have common solvent, and then be merged using crosslinking agents or direct crosslinking of the components [3,17].

Due to their capacity to attract both hydrophilic and hydrophobic substances, APCNs have diverse applications across numerous fields. They are extensively utilized in drug delivery systems, facilitating precise and controlled release by encapsulating and transporting both water-soluble and insoluble drugs [15]. In the realm of biomaterials, they contribute to crafting surfaces that interact favorably with biological elements, supporting advancements in tissue engineering and implants. Some reasons why they are considered advantageous in relation to other materials are [16]:

A) Biocompatibility of these materials can be tailored to mimic biological environments, making them a suitable alternative for implants, drug delivery systems, and tissue engineering without causing adverse reactions within the body.

B) Targeted delivery is related to their capacity to encapsulate both water-soluble and insoluble substances, which allows for accurate and regulated administration of therapeutic agents/drugs to targeted areas, improving the efficacy of drugs while reducing potential side effects.

C) Controlled release is also an important aspect of APCNs, because hey enable the regulated dispensing of drugs or bioactive molecules, ensuring a consistent and prolonged therapeutic impact, which is vital for managing chronic conditions or aiding in tissue regeneration.

D) Versatile design, as explained before, means the high variety of possible synthesis methods, which provides APCNs the possibility of customization for various biomedical applications by ensuring biocompatibility.

APCNs also serve in coatings, forming protective layers with unique wetting properties [17,18], and in environmental remediation, aiding in tasks like oil spill cleanup by regulating the oil/water interface mobility and altering the viscosity of heavy oils [19].

One of the most interesting APCNs is poly(methacrylic acid)-*l*-polyisobutylene (PMAA-*l*-PIB). The PMAA component in these conetworks is an anionic polyelectrolyte which cannot be molded and has high water sensitivity. It has a glass transition temperature between 403 and 458 K depending on the molecular weight of the sample. This is a biocompatible polymer, and used already in drug formulations, such as Eudragit® polymers and their compositions, to prevent decomposition of acid sensitive drugs in the stomach. The three most commonly used preparation techniques to obtain PMAA are free radical polymerization of methacrylic acid in water or methyl ethyl ketone, hydrolysis of poly(methacrylic anhydride) and hydrolysis of esters [20]. Its applications as homo- and copolymer are quite diverse, ranging from pH sensors [21], drug delivery [22] and metal ion removal [23]. However, PMAA's applications are limited by its low chemical and physical resistance. The other component is polyisobutylene (PIB), which is a fully saturated, highly hydrophobic polymer with high chemical and mechanical resistance, with a glass transition temperature in the range of 210 K. Its molecular structure, excellent impermeability to gases and moisture, and biocompatibilty makes it valuable in different fields of applications, such as the inner liner of tubeless tires and biomedical devices. PMAA-*l*-PIB is an APCN previously reported in various research papers [24,25,27,38].

Due to the lack of a common solvent between MAA and PIB, the free radical macromonomer method was employed using methacrylate-telechelic PIB (MA-PIB-MA) previously synthesized in the Polymer Chemistry Research Group and (trimethylsilyl)methacrylate (TMSMA) as starting materials and azobis(isobutyronitrile) (AIBN) as initiator in tetrahydrofuran (THF). This was followed by the removal of the TMS protecting group by HCl solution, which leads to the the desired MAA monomer units in the conetwork. At the end of the synthesis, the result is an APCN that contains PIB as its lipophilic part, which provides mechanical and chemical stability to the sample, along with PMAA as hydrophilic component [24].

II.2. Swelling of crosslinked polymers

The swelling degree or the swelling ratio pertains to the expansion in mass, volume or dimensions of a substance caused by absorbing a solvent. When a solvent interacts favorably with a polymer, it leads to the solvation of polymer chains. The stretching occurs due to factors like crosslinking density, network architecture, and the interaction between the polymer and solvent, resulting in a mechanical force acting upon the stretched polymer [28]. Its measurement helps to comprehend how polymers interact with different solvents and reveals information about the polymer's structure, porosity, and its response to external conditions. The knowledge of swelling behavior is crucial in environmental applications, especially in the context of absorbent materials used in waste management, pollution control or biomedicine.

According to the Flory-Rehner theory, one of the most well-known models based on the Gaussian chain model, when a polymer faces a swelling process in a favorable solvent, there are two forces that govern the process, the elastic energy required to stretch the polymer chains and the mixing free energy associated with the polymer and solvent. The elastic section of the free energy is determined by the chains that are effective in elasticity, significantly affected by the structure, concentration during preparation, and concentration during measurement of the initial polymer [29]. In contrast, the mixing segment of free energy is controlled by osmotic pressure, exclusively affected by the polymer concentration during measurement.

Figure 2 represents the two phenomena which occur simultaneously during the swelling process. On the one hand, the solvent molecules (blue circles) enter the polymer matrix and occupy more and more volume within the sample, while the crosslinks (red circles) move further apart until the equilibrium is reached. This increase in volume generates an accumulation of elastic energy in the crosslinked polymer matrix.

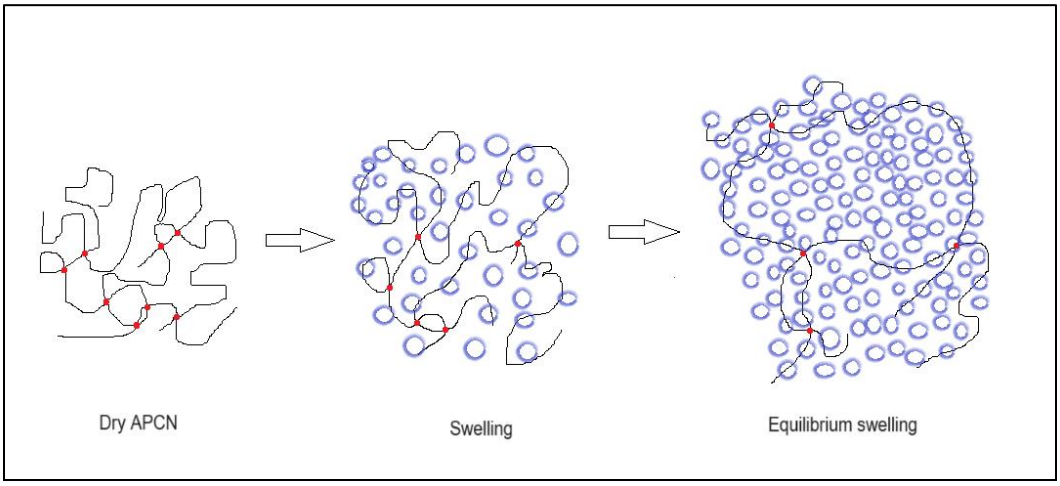

Figure 2. Schematic diagram of the swelling process of polymer networks from the dry state until it reaches the swelling equilibrium

To carry out a swelling study, it is necessary to determine the initial dry mass (or volume) of the polymer network to be analyzed. Then, the network is immersed in a desired solvent for a predetermined time period, followed by weighing to determine the mass of the swollen polymer network. The equation used for the determination of the swelling degree (Q) is the following:

$$Q = \frac{m_t - m_d}{m_d} \qquad (1)$$

where m_d and m_t represent the weights of the dry and swollen networks, respectively.

Amphiphilic conetworks from low, that is, few percent, to very high (over 1000%) swelling capacity in both hydrophilic and hydrophobic solvents have already been reported in the literature [13,24,25,38]. Because of the presence of a relatively large fraction of hydrophobic polymer component in APCNs, their swelling behavior and mechanical properties in aqueous media are especially important. However, according to the best of our knowledge, systematic mechanical property investigations of swollen APCNs have not been reported in the literature so far.

II.3. Elastic modulus of polymer networks

The elastic modulus, also known as Young's modulus, is a measure of a material's stiffness or its resistance to being deformed when a force is applied. It describes how much a material will deform under stress and then return to its original shape once the stress is removed. It is determined by comparing stress to strain within a material's elastic limit. The elastic modulus (*E*) reflects the relationship between stress (σ), which represents the force applied over a specific area, and strain (ε), indicating the resulting deformation or change in length relative to the original length.

$$\sigma = \frac{m_{def} * g}{A} \qquad (2)$$

Stress can be represented as force/area, which taking into consideration Newton's second law, generates the result presented in equation 2, where m_{def} is the load expressed in Kilograms, *g* is the gravity and *A* is the area. Using the Neo-Hookean model, the relative strain (λ) is defined as the difference between the size of the strain (*l*) and the initial height of the sample (l_o). To obtain the elasticity modulus (*E*), the stress values are plotted as a function of $-\left(\lambda - (1/\lambda^2)\right)$, and the slope of the line generated by the linear fit is the modulus of elasticity [30].

The crosslinks of APCNs keep the strands of the polymer chains from displacing very far from their initial positions during a disturbance and prevent the flow of polymer strands relative to each other, thus the material can recover its original structure [31]. Controlling the elastic modulus of APCNs is crucial across numerous applications, allowing tailoring of mechanical properties to match the requirements of specific biological, medical, or engineering contexts. By adjusting the modulus, APCNs can be optimized to interact effectively with biological systems or fulfill mechanical functions in various applications.

II.4. The Korsmeyer-Peppas evaluation of swelling

The Korsmeyer-Peppas model is utilized for explaining the liberation of substances, such as drugs, from and the diffusion of solvents in polymeric structures. It is especially used for scenarios where the discharge process does not neatly fit into traditional models such as Fickian diffusion or zero-order kinetics [32].

$$\frac{m_t - m_0}{m_0} = Kt^n \qquad (3)$$

Equation 3 represents Korsmeyer-Peppas equation, where m_t and m_0 represent the mass of the swollen and dry materials over time (t), respectively, K is defined as the swelling constant, and finally n is the swelling exponent. The value of n can provide the following interpretation [33]:

- n = 0.5, Fickian diffusion – controlled release in case of encapsulated drugs;
- 0.5 < n < 1, non-Fickian or anomalous transport, indicating a diffusion and another mechanism (swelling, erosion, relaxation of polymer chains) which contribute to release;
- n = 1, characteristic of the so called case II transport which indicates a zero-order release kinetics for drugs encapsulated in gels;
- n > 1, might involve a super case II transport that suggest a combination of the swelling, erosion, relaxation of polymer chains, etc.

The Korsmeyer-Peppas model finds wide application in pharmaceutical sciences for comprehending and forecasting the discharge of drugs from diverse formulations like tablets, capsules, patches, salts, and nanoparticles [34]. It empowers researchers to scrutinize and enhance drug delivery systems by gaining insights into the kinetics of swelling, drug release and the underlying mechanisms.

II.5. Diffusion coefficients

Diffusion is the process by which molecules, particles or substances move from areas of higher concentration to areas of lower concentration, driven by the natural tendency of particles to spread out and reach equilibrium. The diffusion coefficients in APCNs involve measuring the rate at which molecules or solutes move in or through the polymer matrix. Some of the principal factors that affect the diffusion coefficient are as follows:

- Amphiphilic nature: Controls how the segments interact with the molecules that diffuse inside the network.
- Network structure: The crosslinking density limits the mobility within the structure. A highly crosslinked polymer tends to have diffusion problems, and in such cases usually the pore size affects the movement of the molecules.

Mathematical models, such as Fick's laws of diffusion or more complex models considering non-Fickian behavior can be implemented to determine the diffusion coefficients. However, other methods like the short time approximation method can also be implemented with relative reliability.

II.6. Effect of salts on polymer gels

The use of several prominent homopolymers or polyelectrolytes in biomedicine and various fields may be limited due to the undesirable interaction that these materials undergo with biologically relevant salts (low or high concentrations). For example, poly(acrylic acid), poly(methacrylic acid) or polyalginates [35,36], when in contact with bi- or multivalent metal ions, present phase transitions, which vary between precipitation and collapse for linear polymers and gels, respectively. Although, these properties may be desired for certain applications, in the biomedical and environmental fields they greatly limit the applicability of these materials. Articles such as the one presented by Horkay et al. describe how hydrogels could be affected with a drastic reduction in their swelling ratio depending on the ion valence and its concentration [37].

The human body contains a variety of ions, and one of the most prevalent ones is sodium ion (Na^+). This is important for nerve function and maintaining fluid balance. Calcium ions (Ca^{2+}) are essential for bone health, muscle contraction, and nerve signaling. Potassium ions (K^+) are crucial for nerve transmission and muscle function.

The interaction between PMAA-*l*-PIB conetworks and the first two mentioned ions, that is, sodium and calcium ions, was analyzed by Kali and Iván [38]. It was found that these conetworks, in contrast to homopolymer polyelectrolyte conetworks [37], do not undergo phase transition or network contraction even at high ion concentration, thus opening its use to possible biomedical applications [38].

III. Goals

As presented in the previous chapter, amphiphilic conetworks (APCNs) belong to a special class of crosslinked polymers, in which otherwise immiscible hydrophilic and hydrophobic polymer are connected to each other by covalent bonds. Swelling these materials in water results in unique hydrogels with relatively high hydrophobic contents. APCNs containing poly(methacrylic acid) as polyelectrolyte hydrophilic component are expected to possess properties which can be utilized in various application fields. While the synthesis of poly(methacrylic acid)-*l*-polyisobutylene (PMAA-*l*-PIB) amphiphilic conetworks is well established, as presented in Section II, the swelling behavior and especially the mechanical properties of these conetworks have not been revealed fully yet. On the basis of these, the major aims of my work are related to the followings:

(1) investigate the swelling of a series of PMAA-*l*-PIB amphiphilic conetworks, samples of which already available in the Polymer Chemistry and Physics Research Group of IMEC, HUN-REN RCNS, in aqueous solution with different pH under constant ionic strength provided by potassium chloride solution;

(2) measure the compression mode stress-strain curves of the PMAA-*l*-PIB APCNs in their state with equilibrium swelling degrees in order to obtain the modulus and its dependence on the composition of the conetworks, the chemical nature of the medium (pH) and the swelling degrees.

IV. Materials, methods and equipment

IV.1. Materials

The PMAA-*l*-PIB APCN samples used in the experiments were prepared previously in the Polymer Chemistry and Physics Research Group of IMEC, HUN-REN RCNS and reported in the MSc Thesis of L. Závoczki [27]. These can be categorized into two groups depending on the polyisobutylene (PIB) used in their synthesis. The samples listed in Table 1 are identified by names beginning with 8 were prepared using PIB with a number average molecular weight of 8,000 g/mol (8k-PIB), while those starting with 10 were obtained using PIB with M_n of 10,000 g/mol (10k-PIB). APCN samples with both kind of PIBs were synthesized with a mass content percentage of 20, 30, 40, 50, 60, 70 m/m% of PIB.

Table 1. Materials used and their provider

Sample name	PIB /PMAA content (m/m%)	Provider
8 - 20	20 / 80	Prepared previously [27]
8 - 30	30 / 70	
8 - 40	40 / 60	
8 - 50	50 / 50	
8 - 60	60 /40	
8 - 70	70 / 30	
10 - 20	20 / 80	
10 - 30	30 / 70	
10 - 40	40 / 60	
10 - 50	50 / 50	
10 - 60	60 / 40	
10 - 70	70 / 30	
Potassium chloride	---	Sigma-Aldrich
Buffer pH (2 ± 0.05)	---	Molar Chemicals
Buffer pH (7 ± 0.05)	---	Molar Chemicals
Buffer pH (10 ± 0.05)	---	Molar Chemicals
H_2O	---	Distilled

IV.2. Swelling measurements

The swelling of the investigated PMAA-*l*-PIB samples were carried in buffer solutions of pH 2, pH 7 and pH 10 containing potassium chloride with 0.05 M concentration in order to provide constant ion strength. On the other hand, due to the physiological importance of potassium ion, information can also be gained on the effect of this ion on the swelling property of the PMAA-*l*-PIB conetworks. The mass of dry samples were measured, and then samples were immersed in the buffer solution. At predetermined time period, the swollen samples were removed, their surface PMAA-*l*-PIB were wiped with a drying paper, and the mass of the sample was measured. Then, the samples were immersed again in the buffer solution. This process was repeated at given times until no significant mass increase was observed. This stage is taken as the equilibrium swelling state.

IV.3. Equipment for modulus measurement

Figure 3. The TA.XTplusC Texture Analyzer [39]

The equipment used for the determination of the elastic modulus of the swollen APCN samples was the TA.XTplusC Texture Analyzer from the Stable Micro Systems brand, which according to the manufacturer tolerates a maximum force of 50 Kg, with speeds between the range of 0.01 to 40 mm/s [39]. It operates by applying selected forces to samples, simulating compression, tension, penetration, or other types of deformation (Figure 3). The stress-strain curves of the APCN samples swollen to equilibrium were measured by compression until 5% of height change was reached. The applied deformation speed was 20 μm/s. The elastic moduli of the samples were obtained by a linear fit on the highest compression range according to literature [42].

V. Results and discussion

V.1. Swelling degrees of PMAA-*l*-PIB conetworks in buffer solutions with different pH

For the determination of swelling degree (Q) measurements, the samples underwent a drying process within an oven under a vacuum environment until achieving a consistent mass. Subsequently, the APCNs were immersed in a 25 ml 0.05 M KCl solution, and their swelling degree over time was meticulously recorded. Considering the dynamic nature of the swelling process, a comprehensive set of measurements was conducted primarily on the initial day of experimentation. Sequential measurements were continued until reaching a state of equilibrium. Furthermore, to investigate the response of the APCNs, the samples were subjected to varying pH environments (pH 2, pH 7, and pH 10).

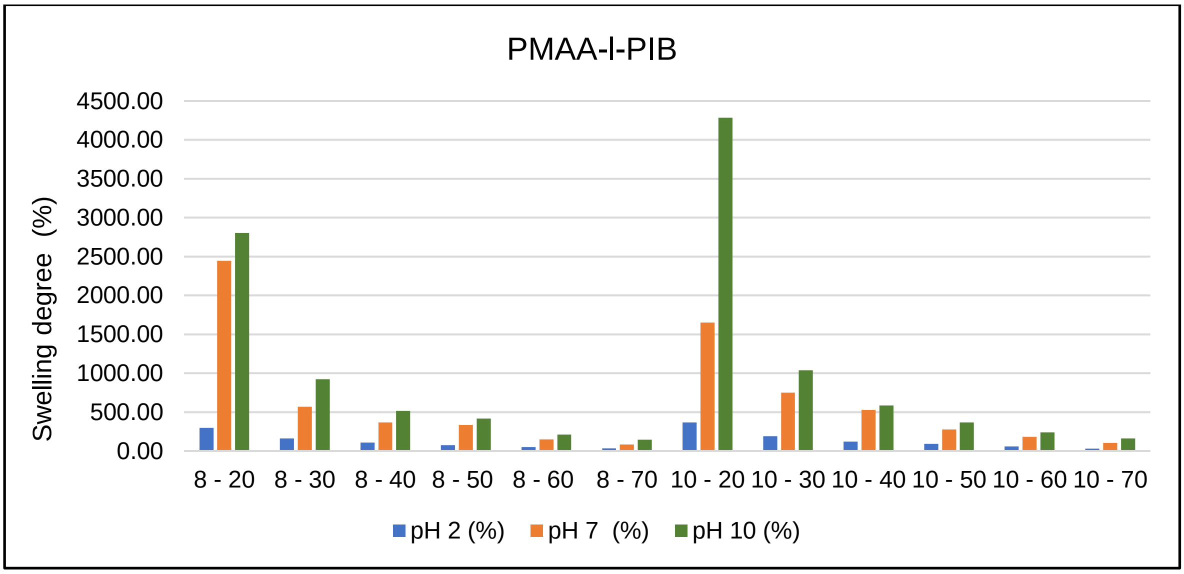

Figure 4. The equilibrium swelling degrees of PMAA-*l*-PIB amphiphilic conetworks in buffer solutions with different pH containing 0.05 M KCl

The swelling degree values were determined by using equation 1. Figure 4 shows the equilibrium swelling degrees for the samples measured at different pH. The presented figure illustrates a notable trend where the equilibrium swelling degree (Q_e) of the APCNs exhibits an increment corresponding to an increase in the solvent's pH, observed consistently within both the 8k and 10k series. The equilibrium swelling degree values obtained at pH 2 and pH 10 have a notable difference of around an order of magnitude. Likewise, the data demonstrates a substantial reduction in the Q_e values as the percentage of PIB increases within the samples, on the one hand. On the other hand, the increase of the pH from acidic (pH 2) to neutral (pH 7) and basic (pH 10) increases the equilibrium swelling degrees significantly. This behavior is due to the increase in dissociated methacrylic acid groups in a basic medium.

Figures 5-7 show the change in mass measured over time for each series (8k left and 10k right) of the swollen PMAA-*l*-PIB conetworks at different pHs. It is important to mention that most of the increase in the swelling degrees occurs during the first two days. From the third day onwards, although the sample is not yet in equilibrium, the percentage of change is not as high as during the first two days. Likewise, it can be clearly observed in these Figures how the percentage of PIB substantially affects the final equilibrium swelling degrees, which are displayed in Figure 5.

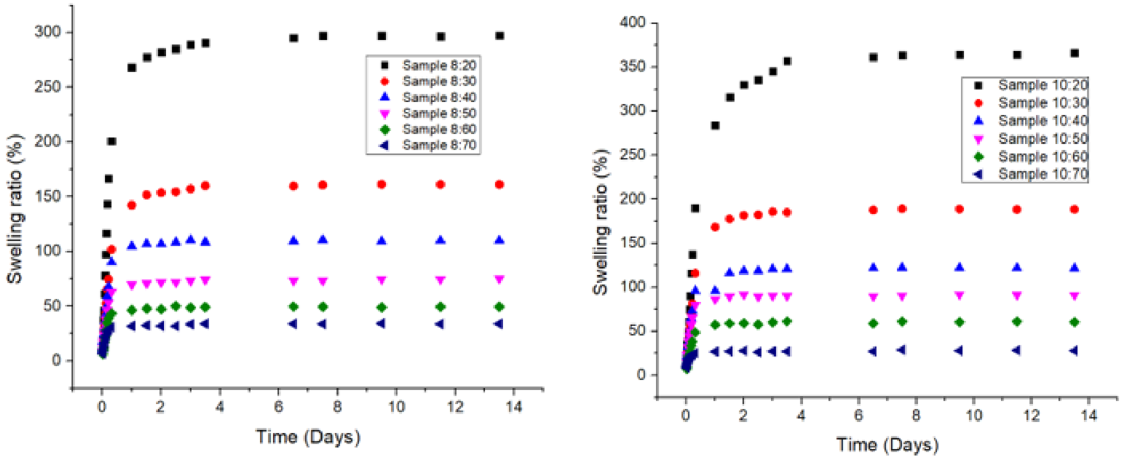

Figure 5. Changes in the swelling degrees of PMAA-*l*-PIB conetworks over time in a pH 2 buffer solution containing 0.05 M KCl

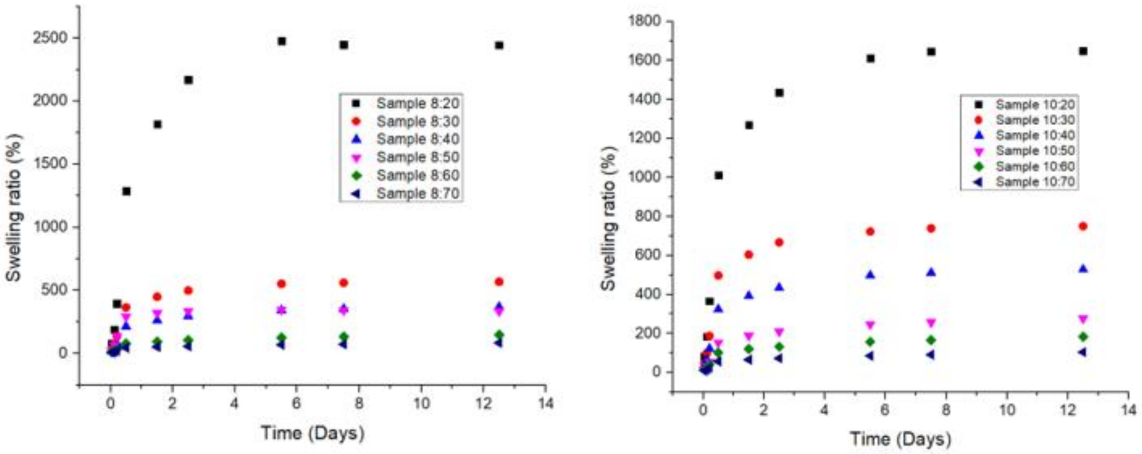

Figure 6. Changes in the swelling degrees of PMAA-*l*-PIB conetworks over time in a pH 7 buffer solution containing 0.05 M KCl

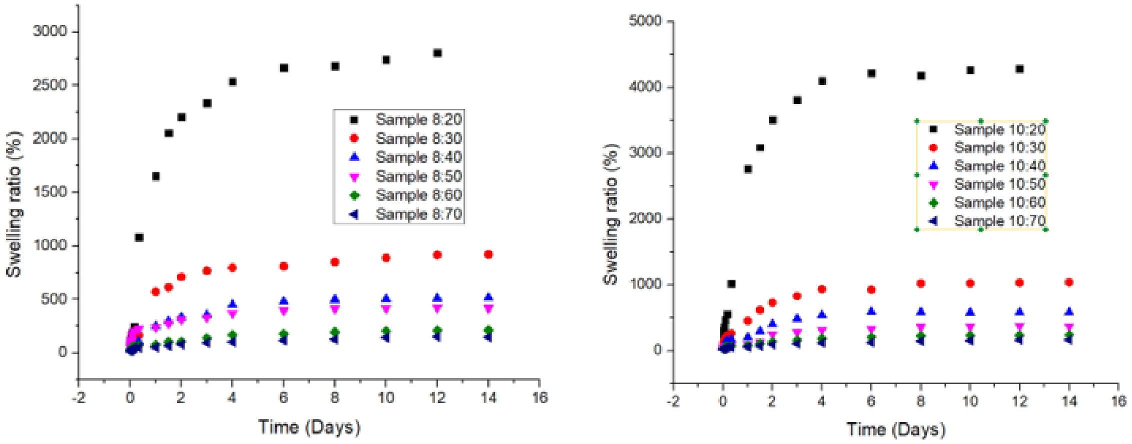

Figure 7. Changes in the swelling degrees of PMAA-*l*-PIB conetworks over time in pH 10 buffer solutions containing 0.05 M KCl

The results of the swelling experiments at pH 2 and 7 agree with those obtained by Závoczki [27] in buffer solutions in the absence of any added salt, like KCl. However, by comparing Figures 8 and 9 for pH 10, we can observe that the swelling degrees of the samples in the presence of KCl, to provide constant ionic strength, is lower significantly than that in a buffer solution without added salt. This is in accordance with our expectations, since the presence of potassium and chloride ions shields the charges of the dissociated methacrylate groups resulting in decreased repulsion, that is, to decreased swelling capacity.

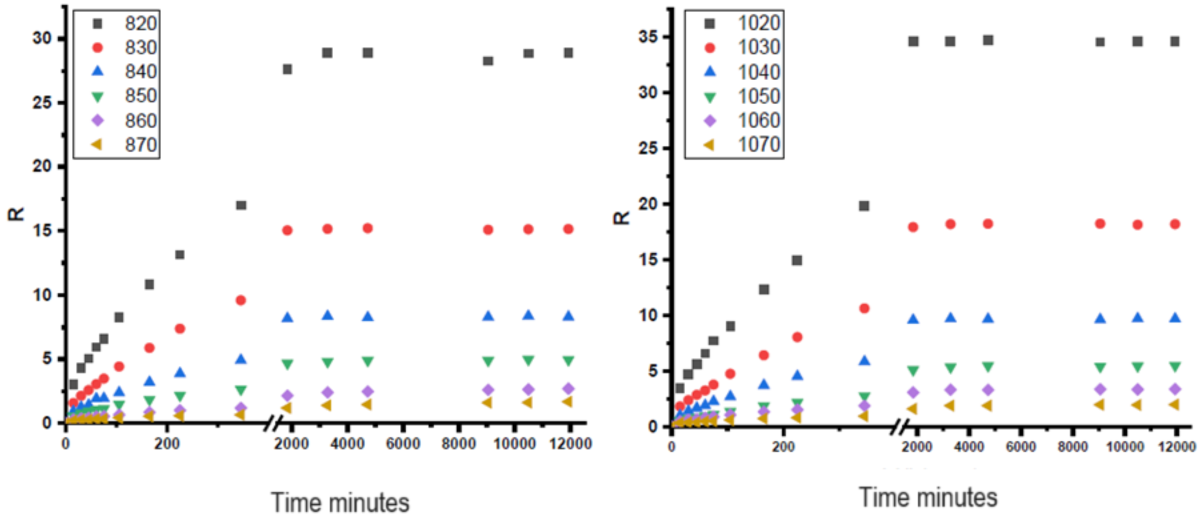

Figure 8. Changes in the swelling degree of PMAA-*l*-PIB conetworks over time in a pH 10 buffer solution without KCl (retrieved from Závoczki [27])

V.2. The evaluation of swelling by the Korsmeyer-Peppas equation

Taking equation 3 as a starting point, we proceed to define the swelling degree (*Q*) as $(m_t - m_0)/m_0$ (see equation 3) and make the following considerations. According to equation 3,

$$Q = K\,t^{n} \quad \text{and thus} \quad lnQ = lnK + n\;lnt$$

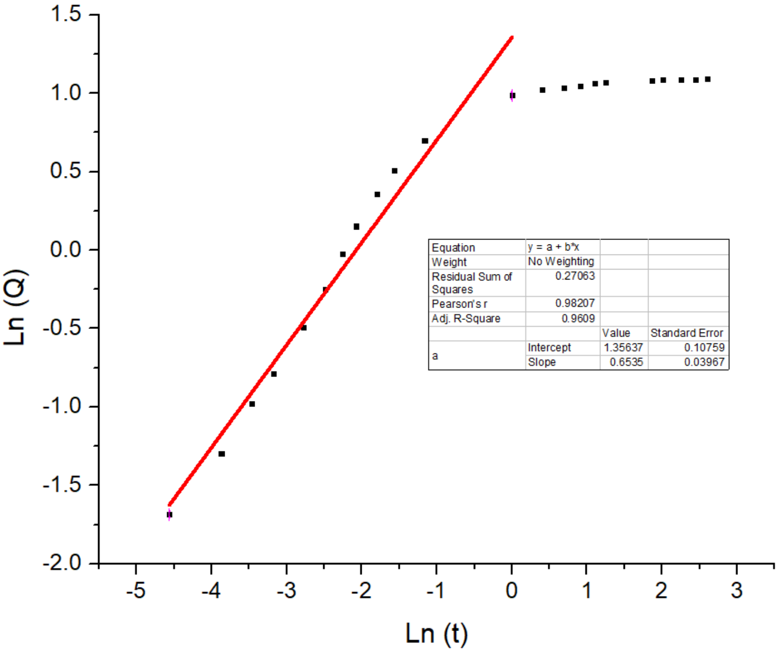

Equation	y = a + b*x		
Weight	No Weighting		
Residual Sum of Squares	0.27063		
Pearson's r	0.98207		
Adj. R-Square	0.9609		
		Value	Standard Error
a	Intercept	1.35637	0.10759
	Slope	0.6535	0.03967

Figure 9. The *lnQ* values as a function of *lnt* in the case of PMAA-*l*-PIB 8-20 at pH 2

Figure 9 shows a representative graph of *lnQ* versus *lnt*, from which the value of *n* and *K* are determined from the slope and the intercept of the linear fitting, respectively. The final swelling degrees at high *Q* values were not taken into consideration since these reflect the equilibrium swelling over time.

The values of *n* and *K* obtained for the samples are shown in Table 2. It can be observed that except for specific exceptions, the value of the swelling exponent and swelling constants decreases as the percentage of PIB increases. With few exceptions, the samples evaluated at pH 2 and 7 present a swelling exponent value greater than 0.5 and less than 1, which denotes a non-Fickian behavior. Fickian diffusion refers to a predictable, linear, and consistent movement of molecules from an area of high concentration to low concentration. However, in many real-world scenarios, especially involving complex materials or systems, the diffusion behavior does not strictly adhere to Fickian principles. Non-Fickian behavior describes situations where the transport mechanism does not fit the classical Fickian diffusion model. These values can be explained as a consequence of the slow relaxation rate of the PMAA-*l*-PIB matrix [40].

Table 2. Swelling exponents and swelling constants of PMAA-*l*-PIB conetworks obtained for swelling at pH 2, 7 and 10 in the presence of KCl (0.05 M)

Sample	pH 2			pH 7			pH 10		
	n	*lnK*	*K*	*n*	*lnK*	*K*	*n*	*lnK*	*K*
8 - 20	0.654	1.356	3.882	0.943	2.786	16.215	0.781	2.759	15.785
8 - 30	0.608	0.572	1.771	0.677	1.260	3.526	0.539	1.513	4.540
8 - 40	0.533	0.325	1.384	0.675	0.726	2.067	0.455	0.814	2.257
8 - 50	0.527	0.010	1.010	0.713	1.202	3.327	0.293	0.966	2.626
8 - 60	0.601	-0.072	0.931	0.502	-0.371	0.690	0.291	-0.054	0.947
8 - 70	0.516	-0.469	0.625	0.522	-0.830	0.436	0.281	-0.419	0.658
10 - 20	0.684	1.266	3.546	0.727	2.292	9.893	0.586	3.088	21.934
10 - 30	0.640	0.726	2.067	0.682	1.563	4.772	0.416	1.618	5.041
10 - 40	0.637	0.667	1.947	0.673	1.133	3.105	0.366	1.041	2.832
10 - 50	0.623	0.566	1.761	0.673	0.386	1.470	0.377	0.419	1.521
10 - 60	0.506	-0.292	0.746	0.591	-0.029	0.971	0.304	0.063	1.065
10 - 70	0.330	-0.916	0.400	0.538	-0.609	0.544	0.277	-0.310	0.734

The values of *n* and *K* obtained for the samples are shown in Table 2. It can be observed that except for specific exceptions, the value of the swelling exponent and swelling constants decreases as the percentage of PIB increases. With few exceptions, the samples evaluated at pH 2 and 7 present a swelling exponent value greater than 0.5 and less than 1, which denotes a non-Fickian behavior. Fickian diffusion refers to a predictable, linear, and consistent movement of molecules from an area of high concentration to low concentration. However, in many real-world scenarios, especially involving complex materials or systems, the diffusion behavior does not strictly adhere to Fickian principles. Non-Fickian behavior describes situations where the transport mechanism does not fit the classical Fickian diffusion model. These values can be explained as a consequence of the slow relaxation rate of the PMAA-*l*-PIB matrix [40].

V.3. Diffusion coefficients of water in swelling the PMAA-*l*-PIB conetworks

To determine the diffusion coefficients, there are experimental methods such as the use of NMR or MRI, fluorescence techniques or steady-state diffusion cells [41], and mathematical modeling methods such as Fick's laws, finite element analysis or curve fitting. The “short time approximation method” is commonly used to determine an approximated value of the diffusion coefficient (*D*) valid only at the first 60% of the swelling degree range of the sample. For a cylindrical sample, generally the following equation is applied.

$$Q = 4\left(\frac{Dt}{\pi r^2}\right)^{1/2} - \pi\left(\frac{Dt}{\pi r^2}\right) - \frac{\pi}{3}\left(\frac{Dt}{\pi r^2}\right)^{\frac{3}{2}} + \ \ldots \quad (4)$$

Where *D* represents the diffusion coefficients in $cm^2\ s^{-1}$, *t* is the time in s, *Q* is the solvent fraction at time *t* in a sample with *r* radius. A semi-empirical relation with the linear fitting was validated by Karadag et al. [32] and Saraydin et al. [40] on acrylamide hydrogels. Figure 10 represents a graph of *Q* versus the square root of time, seeking to obtain as a result the slope which provides the diffusion coefficient of water in the sample. Taking into consideration that the model considers only up to 60% of the swelling degrees, the values that were used for the determination of the diffusion coefficient are those belonging to the first day of swelling of the samples since it is the period where a greatest increase in the swelling degree is recorded.

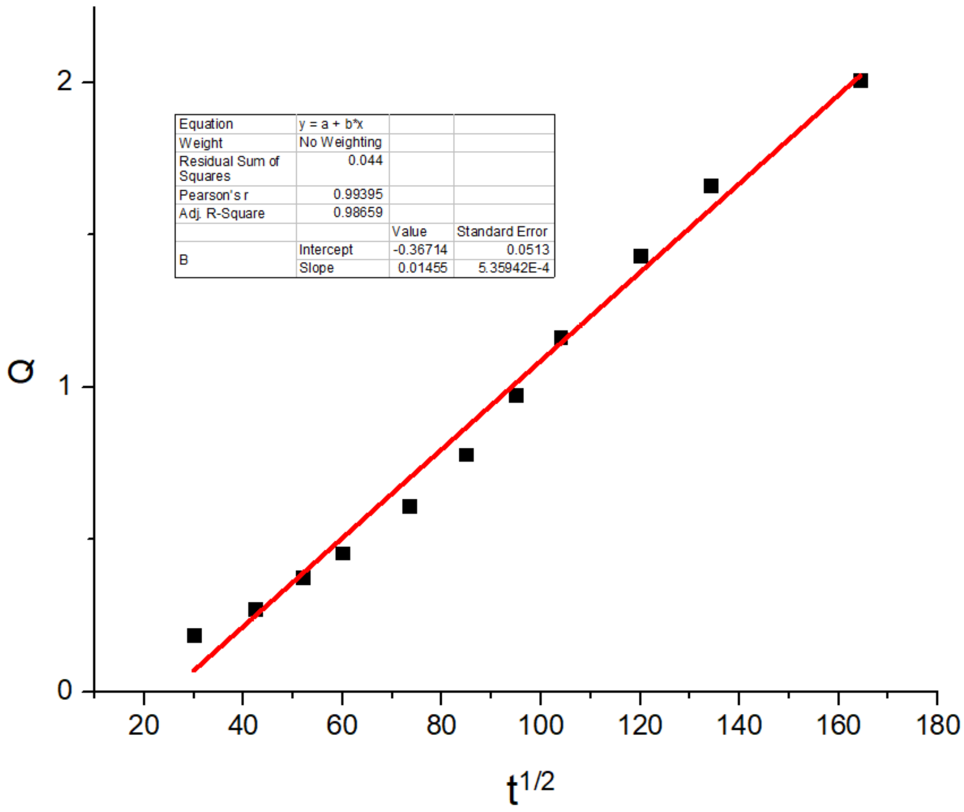

Equation	y = a + b*x		
Weight	No Weighting		
Residual Sum of Squares	0.044		
Pearson's r	0.99395		
Adj. R-Square	0.98659		
		Value	Standard Error
B	Intercept	-0.36714	0.0513
	Slope	0.01455	5.35942E-4

Figure 10. The swelling degree (*Q*) as a function of the square root of swelling time of PMAA-*l*-PIB 8-20 sample swollen at pH 2

Table 3. The diffusion coefficients (in $cm^2 s^{-1} \times 10^6$) of water into PMAA-*l*-PIB conetworks during swelling at pH of 2, 7 and 10

Sample	pH 2	pH 7	pH 10
8 - 20	14.55	62.87	65.38
8 - 30	6.7	14.82	8.66
8 - 40	5.75	8.7	5.42
8 - 50	4.29	10.23	12.61
8 - 60	3.01	2.9	3.29
8 - 70	2.06	1.58	2.19
10 - 20	12.87	42.68	56.62
10 - 30	7.59	20.04	13.37
10 - 40	6.32	12.99	8.69
10 - 50	5.32	6.24	4.04
10 - 60	3.12	3.82	3.21
10 - 70	1.3	2	2.18

Table 3 presents the diffusion coefficients of the APCNs at different pH ranges. As with Figure 10, only the measurements made during the first day of swelling were taken into consideration due to the model restrictions. The values obtained vary between the range of 1.3 to 65.4 (x 10^{-6} cm^2/s), belonging to a pH of 2 with 70% PIB and a pH of 10 with 20% PIB respectively. This confirms that the rate of diffusion of water is higher for PMAA-*l*-PIB with low PIB contents and in solutions with higher pH values.

V.4. Elastic modulus of the swollen PMAA-*l*-PIB conetworks

To assess the elastic modulus, samples at equilibrium swelling degrees were selected. The determination of the samples' perpendicular surface diameter, along with the compression direction's height, was carried out right after removing the samples from the solvent. The highest deformation for all the samples was set at 5% of their total height, and the continuous deformation speed used was 20 μm/s. To prevent the samples from sticking to the machine, the surface perpendicular to the direction of compression was covered with Teflon tape. The test was repeated until three almost identical curves were obtained for each sample. The procedure was maintained for all samples at both pH 2 and pH 7. The diameter and area details of the APCNs analyzed are shown in Tables 6 and 7 in the Appendix section.

In Figure 11, we can see the stress versus $-(\lambda - (1/\lambda^2))$ plot of PMAA-*l*-PIB 8-20 at pH 2. A linear fitting is applied for the larger stress-strain data range for the three curves and the slope is determined using Origin Pro. As shown by Lee et al. [42], the values of the first range of the curves are discarded until a linear behavior is evident in the graph. Additionally, to facilitate the visualization of the linear fitting, the curves have been vertically moved. The stress-strain curves of the rest of the swollen PMAA-*l*-PIB conetwork samples are shown in Figures 14-36 in the Appendix.

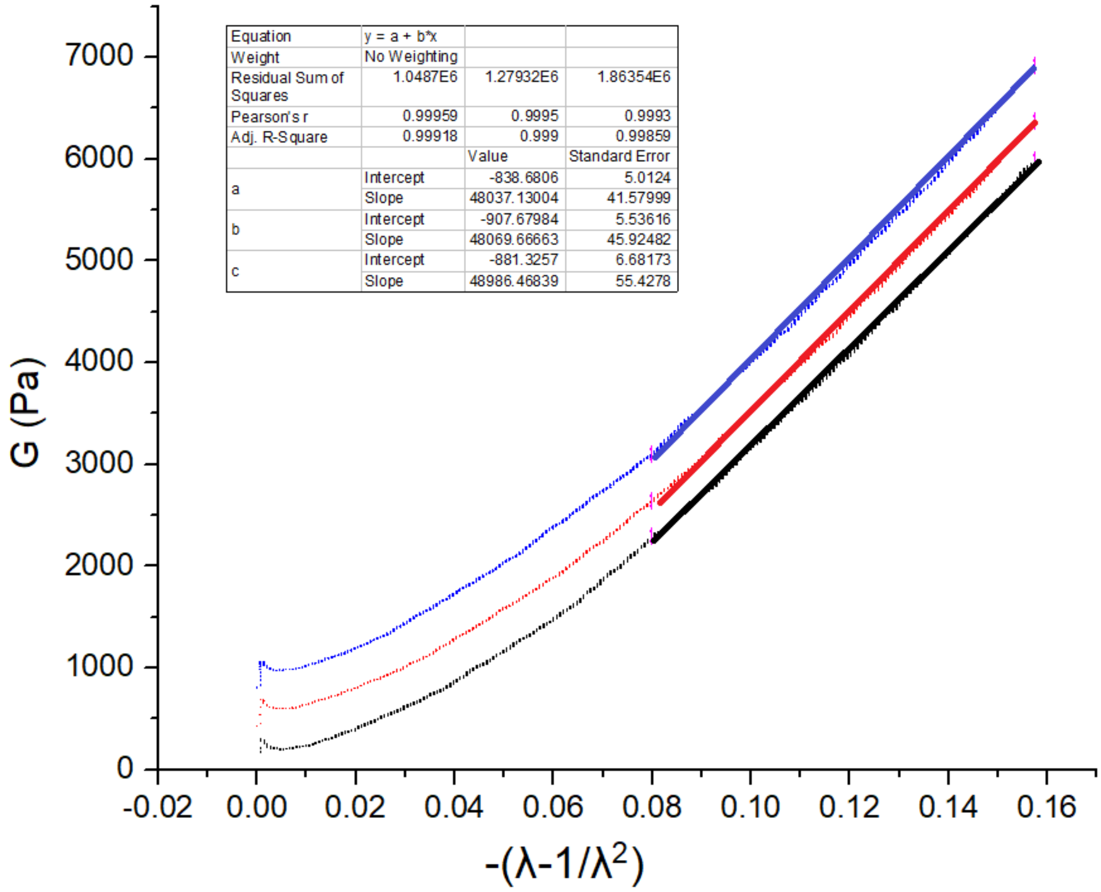

Equation	y = a + b*x		
Weight	No Weighting		
Residual Sum of Squares	1.0487E6	1.27932E6	1.86354E6
Pearson's r	0.99959	0.9995	0.9993
Adj. R-Square	0.99918	0.999	0.99859
		Value	Standard Error
a	Intercept	-838.6806	5.0124
	Slope	48037.13004	41.57999
b	Intercept	-907.67984	5.53616
	Slope	48069.66663	45.92482
c	Intercept	-881.3257	6.68173
	Slope	48986.46839	55.4278

Figure 11. The deformation curves of the PMAA-*l*-PIB-820 sample swollen at pH 2

Table 4 shows the elastic modulus values of the PMAA-*l*-PIB APCNs swollen at pH 2. Each sample has three measurements (a, b and c), and an average of these measurements and the standard deviation are presented. The same procedure is maintained for the samples swollen by a buffer solution with pH 7 and (Table 5).

Table 4. The elastic moduli of PMAA-*l*-PIB conetworks swollen at pH 2

Sample	Elastic modulus (MPa)				
	a	b	c	Average	Standard deviation
8 - 20	0.048	0.048	0.049	0.048	4.40E-04
8 - 30	0.151	0.153	0.159	0.154	3.49E-03
8 - 40	0.649	0.673	0.701	0.674	2.13E-02
8 - 50	0.554	0.569	0.580	0.568	1.08E-02
8 - 60	1.082	1.108	1.116	1.102	1.47E-02
8 - 70	1.206	1.235	1.247	1.229	1.69E-02
10 - 20	0.015	0.016	0.017	0.016	4.80E-04
10 - 30	0.148	0.152	0.164	0.154	6.95E-03
10 - 40	0.446	0.467	0.474	0.462	1.18E-02
10 - 50	0.883	0.904	0.937	0.908	2.22E-02
10 - 60	1.105	1.136	1.147	1.129	1.75E-02
10 - 70	1.615	1.631	1.651	1.632	1.46E-02

Table 5. The elastic moduli of PMAA-*l*-PIB conetworks swollen at pH 7

Sample	Elastic modulus (MPa)				
	a	b	c	Average	Standard deviation
8 - 20	0.002	0.002	0.002	0.002	3.90E-05
8 - 30	0.008	0.008	0.008	0.008	2.79E-04
8 - 40	0.032	0.034	0.036	0.034	2.09E-03
8 - 50	0.023	0.024	0.023	0.024	6.84E-04
8 - 60	0.097	0.107	0.119	0.107	1.10E-02
8 - 70	0.135	0.139	0.142	0.139	3.17E-03
10 - 20	0.003	0.003	0.003	0.003	4.66E-05
10 - 30	0.018	0.018	-------	0.018	4.58E-04
10 - 40	0.032	0.034	0.035	0.034	1.79E-03
10 - 50	0.044	0.046	0.049	0.046	2.37E-03
10 - 60	0.078	0.082	0.084	0.081	3.01E-03
10 - 70	0.154	0.165	0.173	0.164	9.68E-03

Figure 12 presents a direct comparison of the elastic moduli of the PMAA-l-PIB samples swollen at pH 2, 5.5 (obtained by Závoczki [27]) and 7. We can clearly observe that, except for some atypical values the elastic modulus of the APCN decreases with increasing pH, this phenomenon is closely related with the swelling degree of the samples, that is, higher the pH of the aqueous solution, lower the modulus.

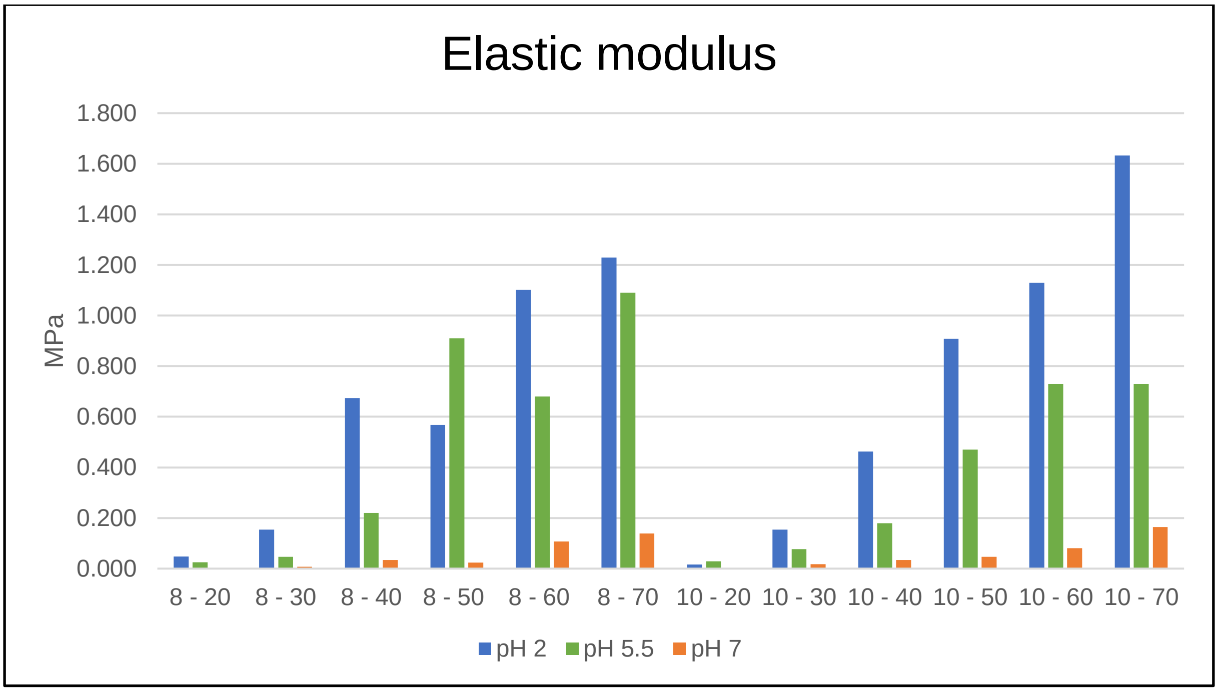

Figure 12. The elastic moduli of PMAA-*l*-PIB conetworks swollen in solutions with pH 2, 5.5 and 7

Increasing the pH, it is observed that the samples retain a greater amount of solvent within their structure, which causes the elastic modulus to decrease, generating an increase in the flexibility and deformation capacity of the APCN. This phenomenon remains stable regardless of the presence of KCl in the sample. However, when increasing the pH to 10 in the presence of KCl (0.05 M), it was observed that the mechanical stability of the swollen PMAA-l-PIB conetwork samples was lost, that is the samples are disintegrated which limits their manipulation. In Figure 13, the PMAA-*l*-PIB8-20 sample swollen at pH 10 is shown after attempting to handle for mechanical test, and it is clearly seen that its structural integrity disappeared, the sample is broken. Therefore, mechanical tests with samples swollen at pH 10 could not be carried out.

Figure 13. The photo on the PMAA-*l*-PIB8-20 sample swollen at pH 10 after its disintegration during the attempt for mechanical test

VI. Summary

Amphiphilic conetworks composed of covalently linked immiscible hydrophilic and hydrophobic polymer chains belong to a relatively new class of rapidly emerging nanophase separated class of materials with various unique application possibilities. Poly(methacrylic acid)-*l*-polyisobutylene (PMAA-*l*-PIB) amphiphilic conetworks (APCNs), one of the most interesting material in this class, having PIB content in the range between 20% and 70%, swollen with potassium chloride (0.05 M) containing aqueous buffer solutions with three different pH (2, 7 and 10) were characterized in terms of their swelling behavior and mechanical properties. The determined quantities were the swelling degrees as a function of swelling time and the elastic modulus. It was found that the equilibrium swelling degrees increase with increasing pH and the hydrophilic PMAA content, that is, decreasing the crosslinking density in these conetworks. During the swelling tests, it was observed that there are two factors which affect the equilibrium swelling degrees, the pH and the composition of these APCNs. The maximum swelling degree was around 4000% with conditions of pH 10 and 20% PIB content in the conetwork, possessing such superabsorbent capacity, which can be utilized in several applications.

The Korsmeyer-Peppas relationship allowed to determine the values of the swelling constant (*K*) and swelling exponent (*n*). These two values in overall are related to the pH value of the buffer solutions and the PIB content in the samples. The higher the pH, these values increase, but on the contrary, increasing the PIB content in the conetworks reduces these values. A high value of *K* indicates a faster diffusion rate of water in the conetworks. The *n* values at pH 2 and 7 indicate a non-Fickian relation, which is presumably due to a combination of diffusion and other mechanisms affecting the swelling of the PMAA-*l*-PIB conetworks by water under the investigated conditions.

The determination of the elastic modulus was carried out by using a linear fitting on a stress versus the $-\left(\lambda - (1/\lambda^2)\right)$ curves obtained for the PMAA-*l*-PIB conetwork samples swollen at pH 2 and 7. It was observed that the elastic modulus decreases with increasing swelling degrees, on the one hand. On the other hand, very broad range of modulus is observed for the swollen PMAA-*l*-PIB conetworks, ranging from 0.002 MPa to 1600 MPa. This interesting result indicates that the strength of the

PMAA-*l*-PIB conetworks can be preliminarily selected in this range depending on the requirements of applications.

The main reasons behind the elastic modulus reduction due to pH increase are the following:

- With increasing pH, ionization (dissociation) of the PMAA component occurs, leading to increased electrostatic repulsion between the polymer chains. This repulsion can cause the conetwork to expand, that is, to swell, leading to a decrease in the elastic modulus. The increased distance between polymer chains reduces their effective interactions, making the material less stiff.
- The pH change can affect the hydration state or the degree of ionization of the acidic functional groups on the polymer chains, leading to changes in chain flexibility and mobility.

The relationships between the composition of the PMAA-*l*-PIB conetworks, their swelling behavior and mechanical properties enable tailored adjustments of the properties of these materials. As a consequence, on the basis of the results of this study, selecting the proper composition for requirements of targeted applications in relation to water uptake and mechanical property (softness) is possible from now on.

VII. References

[1] BBC, “La Edad del Plástico: ¿es este material el que marca el inicio del Antropoceno?,” *BBC News Mundo*, p. 3, 2019, [Online]. Available: https://www.bbc.com/mundo/noticias-49614442.

[2] BBC, “Plastic pollution: Is the drinks industry doing enough to reduce single-use plastics?,” *Newsround*, p. 3, 2021.

[3] M. Weber and R. Stadler, “Hydrophilic-hydrophobic two-component polymer networks: 1. Synthesis of reactive poly(ethylene oxide) telechelics,” *Polymer (Guildf).*, vol. 29, no. 6, pp. 1064–1070, 1988, doi: 10.1016/0032-3861(88)90016-X.

[4] D. Chen, J. P. Kennedy, and A. J. Allen, “Amphlphilic networks. 1. network synthesis by copolymerization of methacryloyl-capped polyisobutylene with 2-(dlmethylamino]ethyl methacrylate and characterization of the networks,” *J. Macromol. Sci. Part A - Chem.*, vol. 25, no. 4, pp. 389–401, 1988, doi: 10.1080/00222338808053376.

[5] C. Patrickios, *Amphiphilic Polymer Co-networks Synthesis, Properties, Modelling and Applications*. The Royal Society of Chemistry, 2020.

[6] J. Li and D. J. Mooney, “Designing hydrogels for controlled drug delivery,” *Nat. Publ. Gr.*, vol. 1, pp. 1–18, 2016, doi: 10.1038/natrevmats.2016.71.

[7] S. Van Vlierberghe, P. Dubruel, and E. Schacht, “Biopolymer-Based Hydrogels As Scaffolds for Tissue Engineering Applications: A Review,” *Biomacromolecules*, vol. 12, no. 5, pp. 1387–1408, May 2011, doi: 10.1021/bm200083n.

[8] G. Savin, N. Bruns, Y. Thomann, and J. C. Tiller, “Nanophase Separated Amphiphilic Microbeads,” pp. 7536–7539, 2005.

[9] G. Kocak, C. Tuncer, and V. Bütün, “pH-Responsive polymers,” *Polym. Chem.*, vol. 8, no. 1, pp. 144–176, 2017, doi: 10.1039/C6PY01872F.

[10] A. Bandzerewicz and A. Gadomska-Gajadhur, “Into the Tissues: Extracellular Matrix and Its Artificial Substitutes: Cell Signalling Mechanisms,” *Cells*, vol. 11, no. 5, 2022, doi: 10.3390/cells11050914.

[11] Y. Osada, J. P. Gong, and Y. Tanaka, “Polymer Gels,” *J. Macromol. Sci. - Polym. Rev.*, vol. 44, no. 1, pp. 87–112, 2004, doi: 10.1081/MC-120027935.

[12] D. E. Apostolides *et al.*, “Near-Model Amphiphilic Polymer Conetworks Based on Four-Arm Stars of Poly(vinylidene fluoride) and Poly(ethylene glycol): Synthesis and Characterization,” *Macromolecules*, vol. 51, no. 7, pp. 2476–2488, 2018, doi: 10.1021/acs.macromol.7b02475.

[13] G. Erdodi and J. P. Kennedy, “Amphiphilic conetworks: Definition, synthesis, applications,” *Prog. Polym. Sci.*, vol. 31, no. 1, pp. 1–18, 2006, doi: 10.1016/j.progpolymsci.2005.11.001.

[14] C. K. Varnava and C. S. Patrickios, “Polymer networks one hundred years after the macromolecular hypothesis : A tutorial review,” *Polymer (Guildf).*, vol. 215, no. December 2020, p. 123322, 2021, doi: 10.1016/j.polymer.2020.123322.

[15] B. Wang *et al.*, “ROS-responsive amphiphilic block copolymer-drug conjugate: Design, synthesis and potential as an efficient drug delivery system via a positive feedback strategy,” *Chem. Eng. J.*, vol. 425, no. July, p. 131453, Dec. 2021, doi: 10.1016/j.cej.2021.131453.

[16] F. Perin, A. Motta, and D. Maniglio, “Amphiphilic copolymers in biomedical applications: Synthesis routes and property control,” *Mater. Sci. Eng. C*, vol. 123, p. 111952, Apr. 2021, doi: 10.1016/j.msec.2021.111952.

[17] T. Kertsomboon and S. Chirachanchai, “Amphiphilic biodegradable co-networks of Poly(butylene succinate)-Poly(ethylene glycol) chains for nano-gelation via Click chemistry and its potential dispersant for multi-walled carbon nanotubes,” *Polym. Degrad. Stab.*, vol. 179, 2020, doi: 10.1016/j.polymdegradstab.2020.109266.

[18] J. Zhang *et al.*, “Transparent amphiphilic silicone-based fouling-release coatings: Analyzing the effect on coating-fouling interfacial behavior,” *Appl. Surf. Sci.*, vol. 641, p. 158532, Dec. 2023, doi: 10.1016/j.apsusc.2023.158532.

[19] H. Yang *et al.*, “A novel active amphiphilic polymer for enhancing heavy oil recovery: Synthesis, characterization and mechanism,” *J. Mol. Liq.*, vol. 391, p. 123210, Dec. 2023, doi: 10.1016/j.molliq.2023.123210.

[20] J. Mark, *POLYMER DATA HANDBOOK*. OXFORD UNIVERSITY PRESS, 1999.

[21] C. Sester, F. Ofridam, N. Lebaz, E. Gagnière, D. Mangin, and A. Elaissari, “pH-Sensitive methacrylic acid–methyl methacrylate copolymer Eudragit L100 and dimethylaminoethyl methacrylate, butyl methacrylate, and methyl methacrylate tri-copolymer Eudragit E100,” *Polym. Adv. Technol.*, vol. 31, no. 3, pp. 440–450, Mar. 2020, doi: 10.1002/pat.4780.

[22] J. Brady, T. Dürig, P. I. Lee, and J.-X. Li, “Polymer Properties and Characterization,” in *Developing Solid Oral Dosage Forms*, Elsevier, 2017, pp. 181–223.

[23] M. A. A. Khalek, G. A. Mahmoud, and N. A. El-kelesh, “Synthesis and Characterization of Poly-Methacrylic Acid Grafted Chitosan-Bentonite Composite and its Application for Heavy Metals Recovery,” pp. 1–13, 2012.

[24] M. Haraszti, E. Tóth, and B. Iván, “Poly(methacrylic acid)- l -Polyisobutylene: A Novel Polyelectrolyte Amphiphilic Conetwork,” *Chem. Mater.*, vol. 18, no. 20, pp. 4952–4958, Oct. 2006, doi: 10.1021/cm061119v.

[25] G. Kali and B. Iván, “Poly (methacrylic acid) - l -Polyisobutylene Amphiphilic Conetworks by Using an Ethoxyethyl-Protected Comonomer : Synthesis , Protecting Group Removal in the Cross-Linked State , and Characterization,” pp. 1–9, 2015, doi: 10.1002/macp.201400478.

[26] S. Pásztor, B. Becsei, Gy. Szarka, Y. Thomann, R. Thomann, M. Mülhaupt and B. Iván, “The Scissors Effect in Action: The Fox-Flory Relationship between the Glass Transition Temperature of Crosslinked Poly(Methyl Methacrylate) and M_c in Nanophase Separated Poly(Methyl Methacrylate)-*l*-Polyisobutylene Conetworks” *Materials (Basel).*, vol. 4822, pp. 1–15, 2020.

[27] L. Závolczki, “Polimetakrilsav-*l*-polizobutilén amfifil kotérhálók előállítása, vizsgálata és nemesfém nanorészecske hordozóként való alkalmazása,” MSc Thesis, Eötvös Loránd Tudományegyetem, 2022.

[28] F. K. Metze, S. Sant, Z. Meng, H. Klok, and K. Kaur, “Swelling-Activated, Soft Mechanochemistry in Polymer Materials,” *Langmuir*, 2023, doi:

10.1021/acs.langmuir.2c02801.

[29] T. Sakai, M. Kurakazu, Y. Akagi, M. Shibayama, and U. Il Chung, “Effect of swelling and deswelling on the elasticity of polymer networks in the dilute to semi-dilute region,” *Soft Matter*, vol. 8, no. 9, pp. 2730–2736, 2012, doi: 10.1039/c2sm07043j.

[30] M. Rubinstein and R. Colby, *Polymer Physics*. Oxford University Press, 2003.

[31] Z. Li, Z. Liu, T. Y. Ng, and P. Sharma, “The effect of water content on the elastic modulus and fracture energy of hydrogel,” *Extrem. Mech. Lett.*, vol. 35, p. 100617, 2020, doi: 10.1016/j.eml.2019.100617.

[32] E. Karadağ, Ö. B. Üzüm, and D. Saraydin, “Swelling equilibria and dye adsorption studies of chemically crosslinked superabsorbent acrylamide/maleic acid hydrogels,” *Eur. Polym. J.*, vol. 38, no. 11, pp. 2133–2141, 2002, doi: 10.1016/S0014-3057(02)00117-9.

[33] D. Wójcik-Pastuszka, J. Krzak, B. Macikowski, R. Berkowski, B. Osiński, and W. Musiał, “Evaluation of the release kinetics of a pharmacologically active substance from model intra-articular implants replacing the cruciate ligaments of the knee,” *Materials (Basel).*, vol. 12, no. 8, 2019, doi: 10.3390/ma12081202.

[34] I. Y. Wu, S. Bala, N. Škalko-Basnet, and M. P. di Cagno, “Interpreting non-linear drug diffusion data: Utilizing Korsmeyer-Peppas model to study drug release from liposomes,” *Eur. J. Pharm. Sci.*, vol. 138, no. July, p. 105026, 2019, doi: 10.1016/j.ejps.2019.105026.

[35] A. Katchalsky and I. Michaeli, “Polyelectrolyte gels in salt solutions,” *J. Polym. Sci.*, vol. 15, no. 79, pp. 69–86, 1955, doi: 10.1002/pol.1955.120157906.

[36] K. Y. Lee and D. J. Mooney, “Alginate: Properties and biomedical applications,” *Prog. Polym. Sci.*, vol. 37, no. 1, pp. 106–126, 2012, doi: 10.1016/j.progpolymsci.2011.06.003.

[37] F. Horkay, I. Tasaki, and P. J. Basser, “Osmotic swelling of polyacrylate hydrogels in physiological salt solutions,” *Biomacromolecules*, vol. 1, no. 1, pp. 84–90, 2000, doi: 10.1021/bm9905031.

[38] G. Kali and B. Iván, “Noncollapsing polyelectrolyte conetwork gels in

physiologically relevant salt solutions,” *Eur. Polym. J.*, vol. 84, pp. 668–674, 2016, doi: 10.1016/j.eurpolymj.2016.10.006.

[39] StableMicroSystems, “TA.XTplusC Texture Analyser,” 2023. https://www.stablemicrosystems.com/TAXTplus.html.

[40] D. Saraydin, H. Nursevin Öztop, E. Karadağ, Y. Çaldiran, and O. Güven, “Influence of some amino acids on the dynamic swelling behavior of radiation-induced acrylamide hydrogel,” *Appl. Biochem. Biotechnol. - Part A Enzym. Eng. Biotechnol.*, vol. 82, no. 2, pp. 115–125, 1999, doi: 10.1385/abab:82:2:115.

[41] S. M. Evans, A. L. Litzenberger, A. E. Ellenberger, J. E. Maneval, E. L. Jablonski, and B. M. Vogel, “A microfluidic method to measure small molecule diffusion in hydrogels,” *Mater. Sci. Eng. C*, vol. 35, no. 1, pp. 322–334, 2014, doi: 10.1016/j.msec.2013.10.035.

[42] D. Lee, H. Zhang, and S. Ryu, “Elastic Modulus Measurement of Hydrogels,” Springer, Cham, 2018, pp. 1–21.

[43] P. J. Flory, "Principles of Polymer Chemistry", Cornell University Press, Ithaca, London, 1953.

VIII. Appendix

Table 6. Parameters used to determine the elastic modulus of PMAA-*l*-PIB at pH 2

Sample	Diameter (mm)	Height (mm)	Area $(mm)^2$
8 - 20	17.70	4.60	246.06
8 - 30	15.85	8.26	197.31
8 - 40	14.55	7.95	166.27
8 - 50	13.35	3.87	139.98
8 - 60	12.57	4.83	124.10
8 - 70	11.98	4.98	112.72
10 - 20	18.23	8.96	261.01
10 - 30	16.54	8.18	214.86
10 - 40	15.02	6.85	177.19
10 - 50	13.63	7.79	145.91
10 - 60	13.10	6.24	134.78
10 - 70	12.16	6.57	116.13

Table 7. Parameters used to determine the elastic modulus of PMAA-*l*-PIB at pH 7

Sample	Diameter (mm)	Height (mm)	Area $(mm)^2$
8 - 20	26.16	9.53	537.48
8 - 30	22.69	8.26	404.35
8 - 40	20.07	7.95	316.36
8 - 50	19.36	3.87	294.37
8 - 60	15.37	4.83	185.54
8 - 70	14.19	4.98	158.14
10 - 20	29.77	8.96	696.06
10 - 30	24.86	8.18	485.39
10 - 40	21.92	6.85	377.37
10 - 50	18.93	7.79	281.44
10 - 60	16.31	6.24	208.93
10 - 70	14.42	6.57	163.31

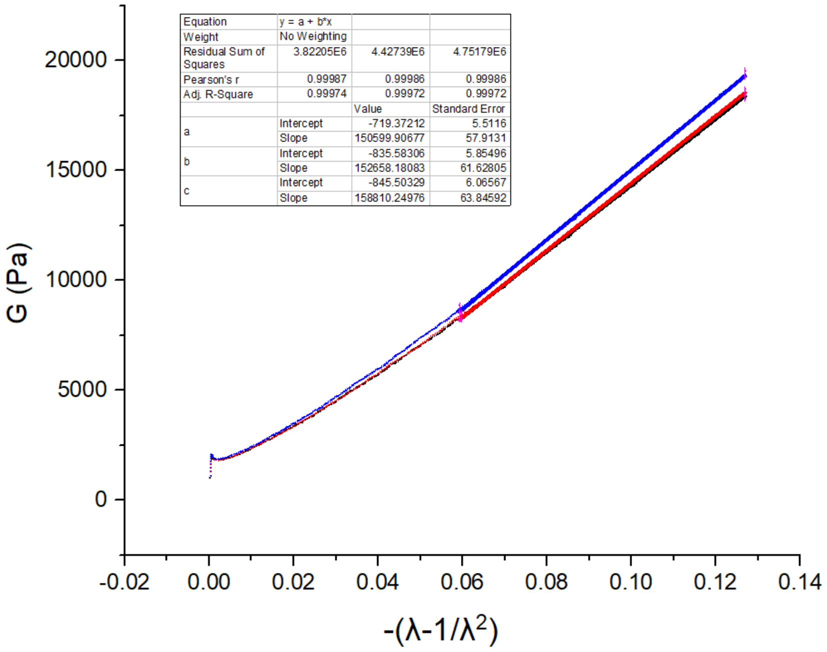

Equation	y = a + b*x		
Weight	No Weighting		
Residual Sum of Squares	3.82205E6	4.42739E6	4.75179E6
Pearson's r	0.99987	0.99986	0.99986
Adj. R-Square	0.99974	0.99972	0.99972
		Value	Standard Error
a	Intercept	-719.37212	5.5116
	Slope	150599.90677	57.9131
b	Intercept	-835.58306	5.85496
	Slope	152658.18083	61.62805
c	Intercept	-845.50329	6.06567
	Slope	158810.24976	63.84592

Figure 14. The deformation curves PMAA-/-PIB-830-pH2

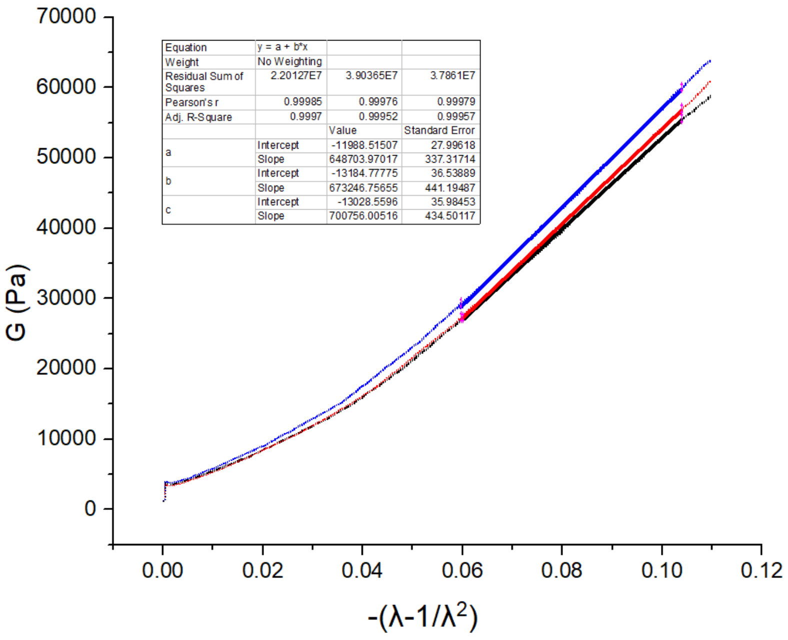

Equation	y = a + b*x		
Weight	No Weighting		
Residual Sum of Squares	2.20127E7	3.90365E7	3.7861E7
Pearson's r	0.99985	0.99976	0.99979
Adj. R-Square	0.9997	0.99952	0.99957
		Value	Standard Error
a	Intercept	-11988.51507	27.99618
	Slope	648703.97017	337.31714
b	Intercept	-13184.77775	36.53889
	Slope	673246.75655	441.19487
c	Intercept	-13028.5596	35.98453
	Slope	700756.00516	434.50117

Figure 15. The deformation curves PMAA-/-PIB-840-pH2

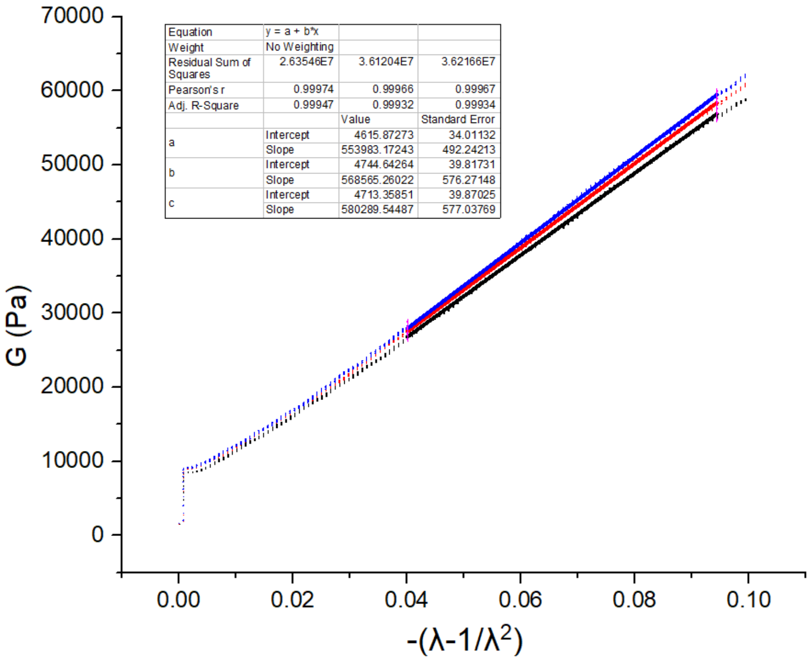

Equation	y = a + b*x		
Weight	No Weighting		
Residual Sum of Squares	2.63546E7	3.61204E7	3.62166E7
Pearson's r	0.99974	0.99966	0.99967
Adj. R-Square	0.99947	0.99932	0.99934
		Value	Standard Error
a	Intercept	4615.87273	34.01132
	Slope	553983.17243	492.24213
b	Intercept	4744.64264	39.81731
	Slope	568565.26022	576.27148
c	Intercept	4713.35851	39.87025
	Slope	580289.54487	577.03769

Figure 16. The deformation curves PMAA-*l*-PIB-850-pH2

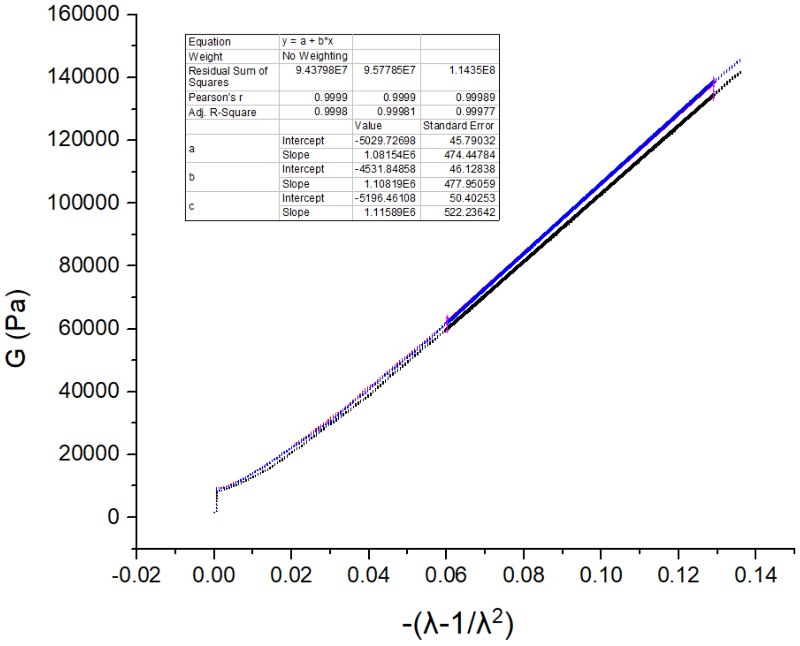

Equation	y = a + b*x		
Weight	No Weighting		
Residual Sum of Squares	9.43798E7	9.57785E7	1.1435E8
Pearson's r	0.9999	0.9999	0.99989
Adj. R-Square	0.9998	0.99981	0.99977
		Value	Standard Error
a	Intercept	-5029.72698	45.79032
	Slope	1.08154E6	474.44784
b	Intercept	-4531.84858	46.12838
	Slope	1.10819E6	477.95059
c	Intercept	-5196.46108	50.40253
	Slope	1.11589E6	522.23642

Figure 17. The deformation curves PMAA-*l*-PIB-860-pH2

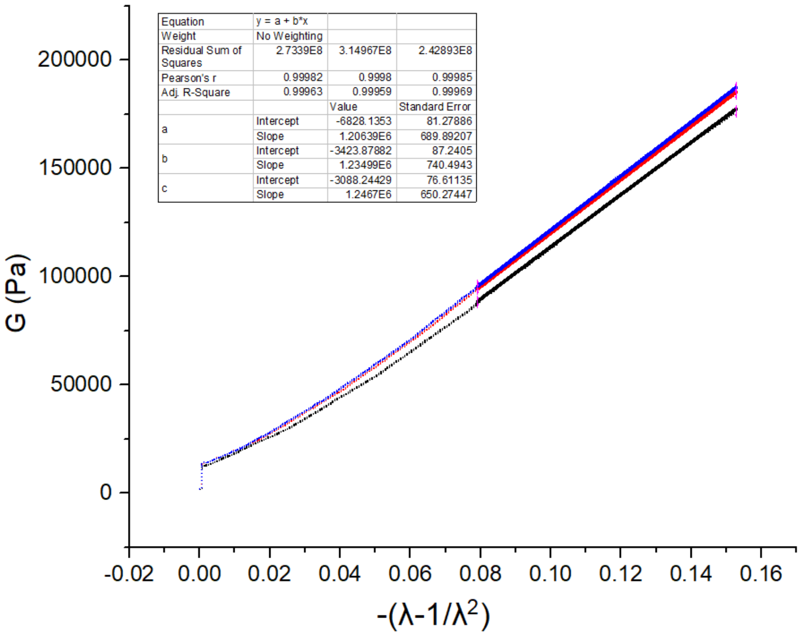

Equation	y = a + b*x		
Weight	No Weighting		
Residual Sum of Squares	2.7339E8	3.14967E8	2.42893E8
Pearson's r	0.99982	0.9998	0.99985
Adj. R-Square	0.99963	0.99959	0.99969
		Value	Standard Error
a	Intercept	-6828.1353	81.27886
	Slope	1.20639E6	689.89207
b	Intercept	-3423.87882	87.2405
	Slope	1.23499E6	740.4943
c	Intercept	-3088.24429	76.61135
	Slope	1.2467E6	650.27447

Figure 18. The deformation curves PMAA-*l*-PIB-870-pH2

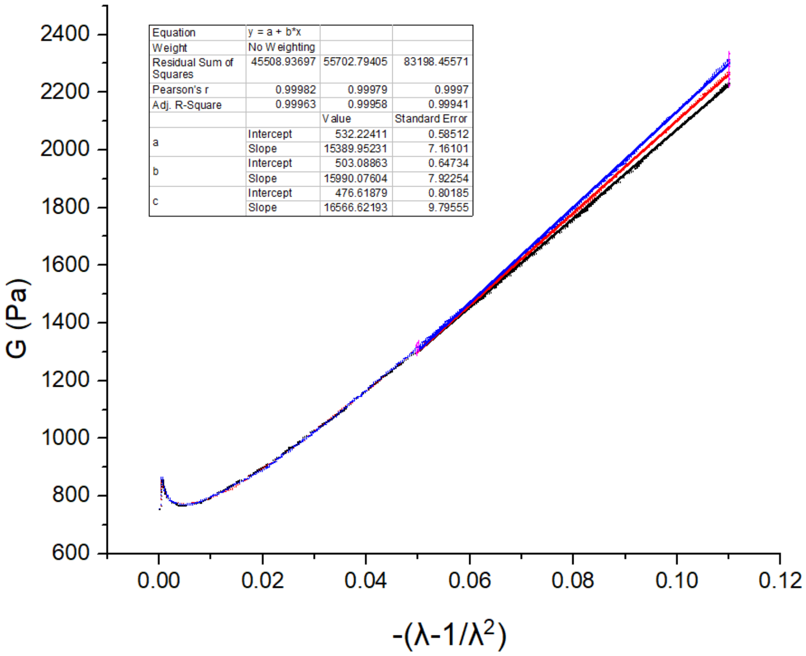

Equation	y = a + b*x		
Weight	No Weighting		
Residual Sum of Squares	45508.93697	55702.79405	83198.45571
Pearson's r	0.99982	0.99979	0.9997
Adj. R-Square	0.99963	0.99958	0.99941
		Value	Standard Error
a	Intercept	532.22411	0.58512
	Slope	15389.95231	7.16101
b	Intercept	503.08863	0.64734
	Slope	15990.07604	7.92254
c	Intercept	476.61879	0.80185
	Slope	16566.62193	9.79555

Figure19. The deformation curves PMAA-*l*-PIB-1020-pH2

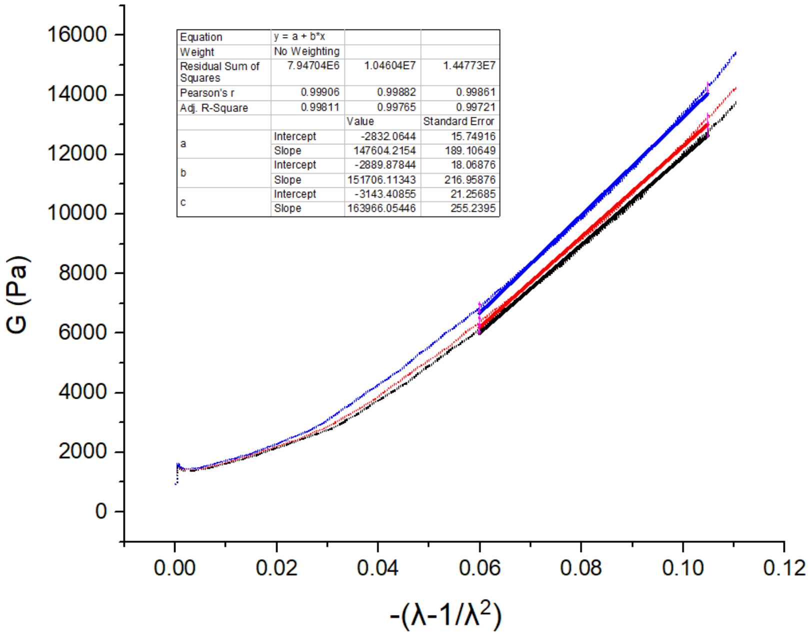

Equation	y = a + b*x		
Weight	No Weighting		
Residual Sum of Squares	7.94704E6	1.04604E7	1.44773E7
Pearson's r	0.99906	0.99882	0.99861
Adj. R-Square	0.99811	0.99765	0.99721
		Value	Standard Error
a	Intercept	-2832.0644	15.74916
	Slope	147604.2154	189.10649
b	Intercept	-2889.87844	18.06876
	Slope	151706.11343	216.95876
c	Intercept	-3143.40855	21.25685
	Slope	163966.05446	255.2395

Figure 20. The deformation curves PMAA-*l*-PIB-1030-pH2

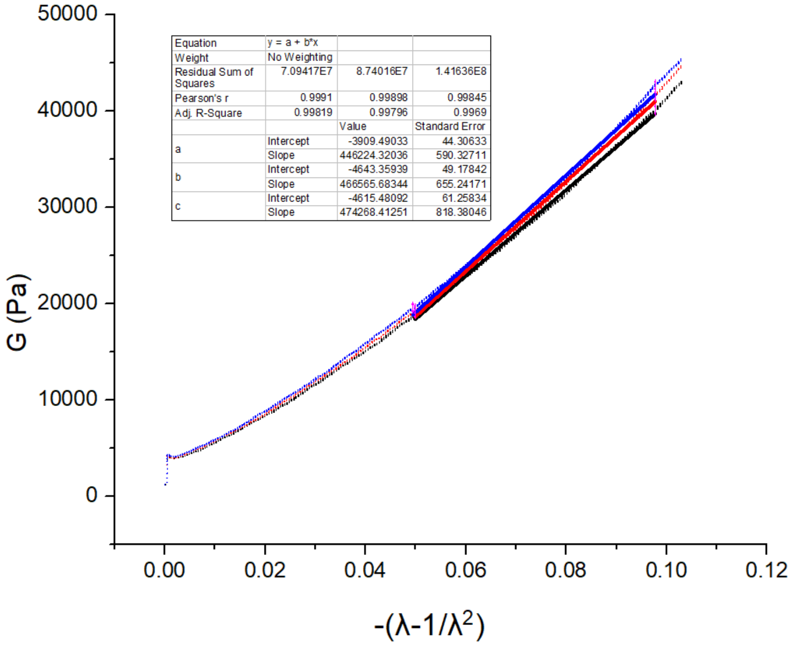

Equation	y = a + b*x		
Weight	No Weighting		
Residual Sum of Squares	7.09417E7	8.74016E7	1.41636E8
Pearson's r	0.9991	0.99898	0.99845
Adj. R-Square	0.99819	0.99796	0.9969
		Value	Standard Error
a	Intercept	-3909.49033	44.30633
	Slope	446224.32036	590.32711
b	Intercept	-4643.35939	49.17842
	Slope	466565.68344	655.24171
c	Intercept	-4615.48092	61.25834
	Slope	474268.41251	818.38046

Figure 21. The deformation curves PMAA-*l*-PIB-1040-pH2

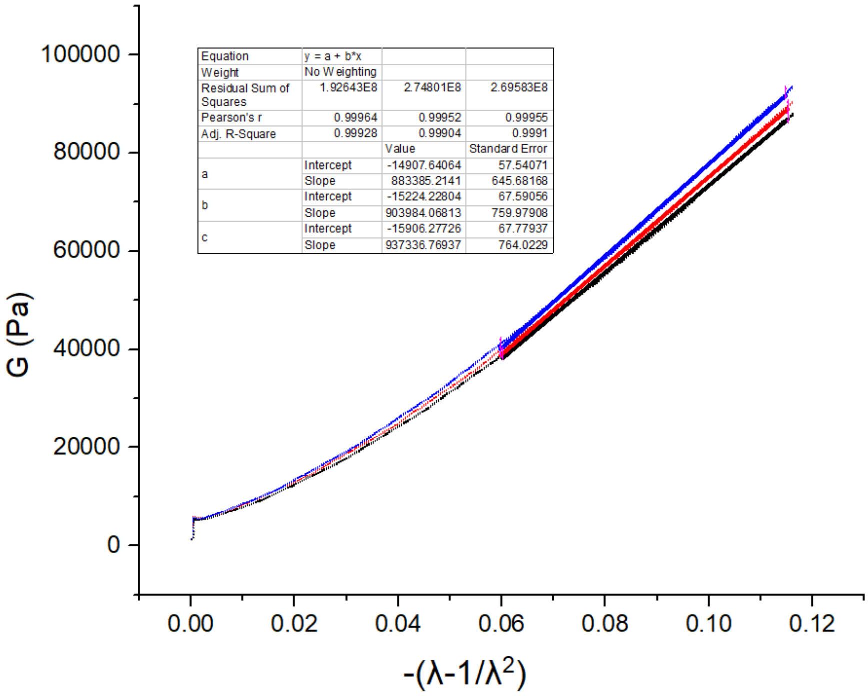

Equation	y = a + b*x		
Weight	No Weighting		
Residual Sum of Squares	1.92643E8	2.74801E8	2.69583E8
Pearson's r	0.99964	0.99952	0.99955
Adj. R-Square	0.99928	0.99904	0.9991
		Value	Standard Error
a	Intercept	-14907.64064	57.54071
	Slope	883385.2141	645.68168
b	Intercept	-15224.22804	67.59056
	Slope	903984.06813	759.97908
c	Intercept	-15906.27726	67.77937
	Slope	937336.76937	764.0229

Figure 22. The deformation curves PMAA-*l*-PIB-1050-pH2

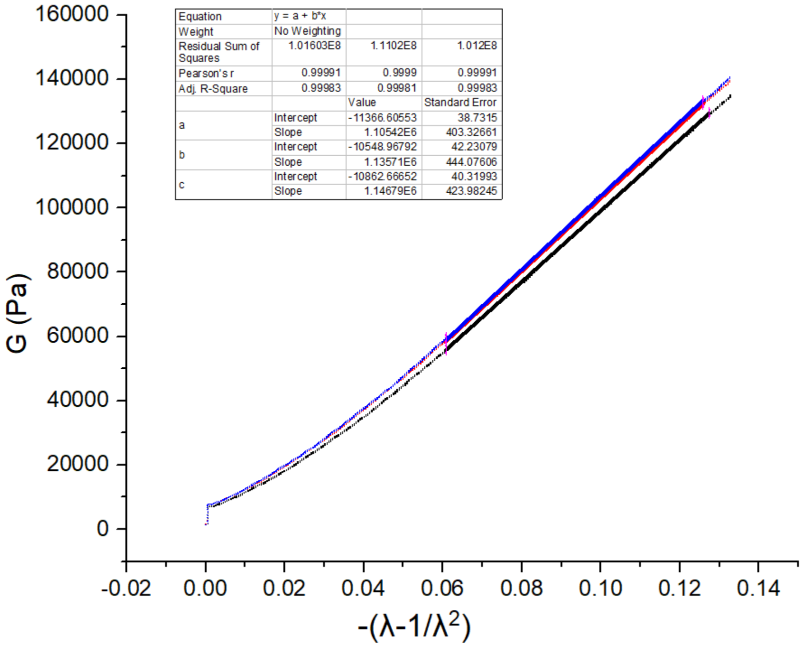

Equation	y = a + b*x		
Weight	No Weighting		
Residual Sum of Squares	1.01603E8	1.1102E8	1.012E8
Pearson's r	0.99991	0.9999	0.99991
Adj. R-Square	0.99983	0.99981	0.99983
		Value	Standard Error
a	Intercept	-11366.60553	38.7315
	Slope	1.10542E6	403.32661
b	Intercept	-10548.96792	42.23079
	Slope	1.13571E6	444.07606
c	Intercept	-10862.66652	40.31993
	Slope	1.14679E6	423.98245

Figure 23. The deformation curves PMAA-*l*-PIB-1060-pH2

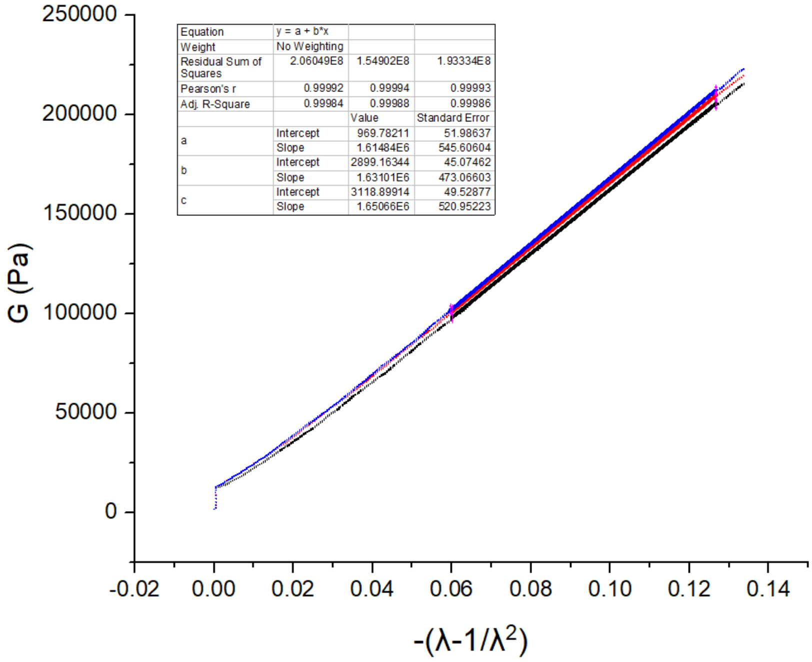

Equation	y = a + b*x		
Weight	No Weighting		
Residual Sum of Squares	2.06049E8	1.54902E8	1.93334E8
Pearson's r	0.99992	0.99994	0.99993
Adj. R-Square	0.99984	0.99988	0.99986
		Value	Standard Error
a	Intercept	969.78211	51.98637
	Slope	1.61484E6	545.60604
b	Intercept	2899.16344	45.07462
	Slope	1.63101E6	473.06603
c	Intercept	3118.89914	49.52877
	Slope	1.65066E6	520.95223

Figure 24. The deformation curves PMAA-*l*-PIB-1070-pH2

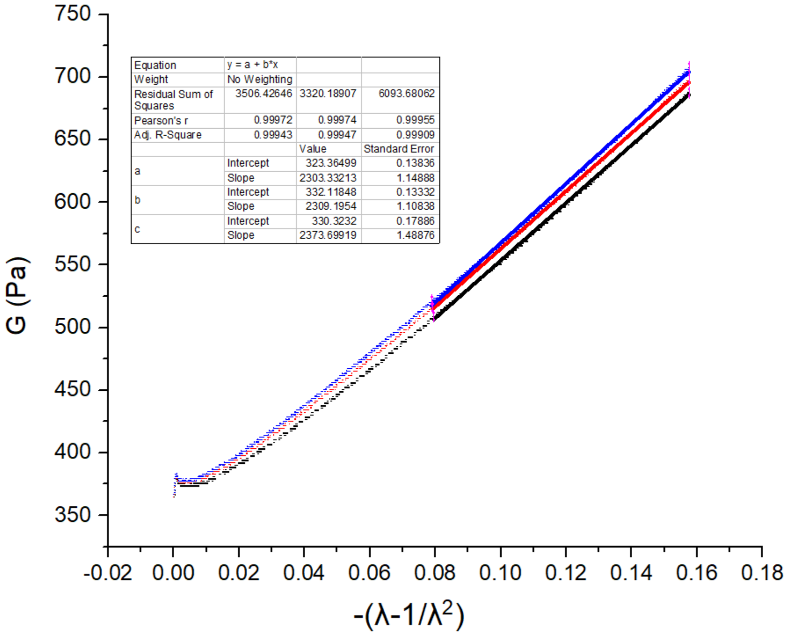

Equation	y = a + b*x		
Weight	No Weighting		
Residual Sum of Squares	3506.42646	3320.18907	6093.68062
Pearson's r	0.99972	0.99974	0.99955
Adj. R-Square	0.99943	0.99947	0.99909
		Value	Standard Error
a	Intercept	323.36499	0.13836
	Slope	2303.33213	1.14888
b	Intercept	332.11848	0.13332
	Slope	2309.1954	1.10838
c	Intercept	330.3232	0.17886
	Slope	2373.69919	1.48876

Figure 25. The deformation curves PMAA-*l*-PIB-820-pH7

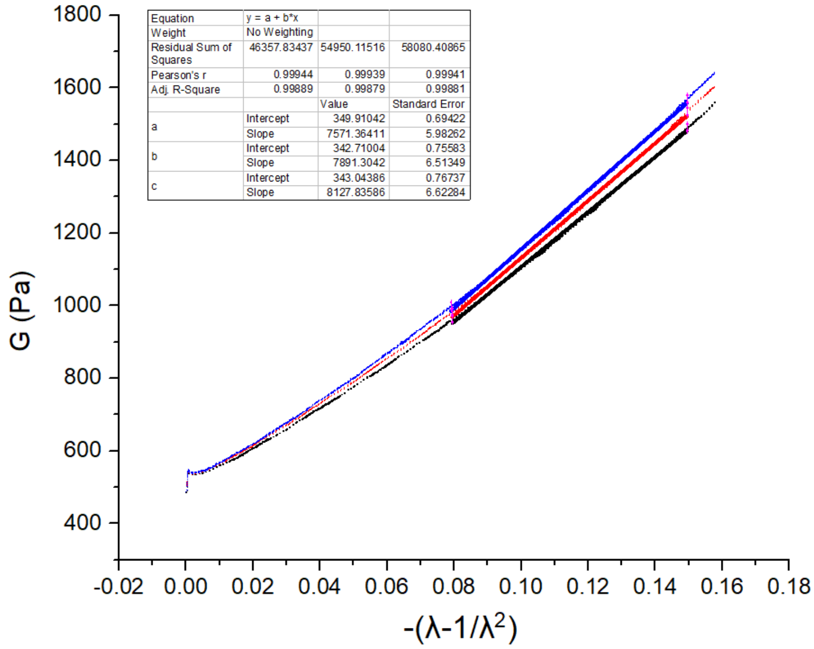

Equation	y = a + b*x		
Weight	No Weighting		
Residual Sum of Squares	46357.83437	54950.11516	58080.40865
Pearson's r	0.99944	0.99939	0.99941
Adj. R-Square	0.99889	0.99879	0.99881
		Value	Standard Error
a	Intercept	349.91042	0.69422
	Slope	7571.36411	5.98262
b	Intercept	342.71004	0.75583
	Slope	7891.3042	6.51349
c	Intercept	343.04386	0.76737
	Slope	8127.83586	6.62284

Figure 26. The deformation curves PMAA-/-PIB-830-pH7

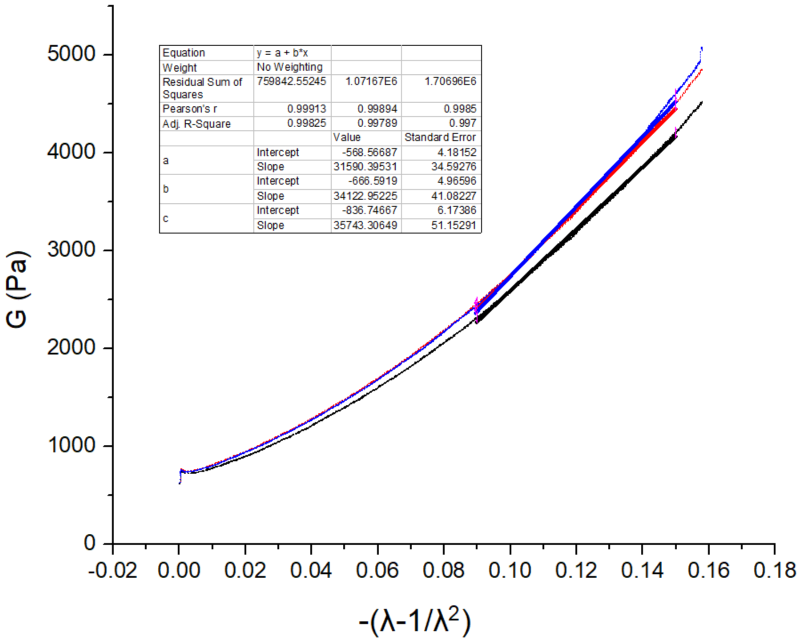

Equation	y = a + b*x		
Weight	No Weighting		
Residual Sum of Squares	759842.55245	1.07167E6	1.70696E6
Pearson's r	0.99913	0.99894	0.9985
Adj. R-Square	0.99825	0.99789	0.997
		Value	Standard Error
a	Intercept	-568.56687	4.18152
	Slope	31590.39531	34.59276
b	Intercept	-666.5919	4.96596
	Slope	34122.95225	41.08227
c	Intercept	-836.74667	6.17386
	Slope	35743.30649	51.15291

Figure 27. The deformation curves PMAA-/-PIB-840-pH7

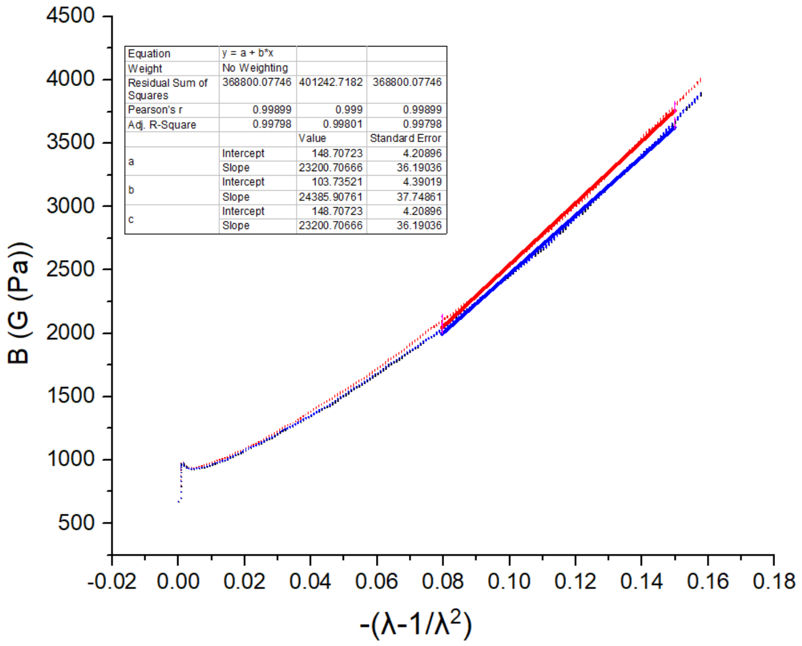

Equation	y = a + b*x		
Weight	No Weighting		
Residual Sum of Squares	368800.07746	401242.7182	368800.07746
Pearson's r	0.99899	0.999	0.99899
Adj. R-Square	0.99798	0.99801	0.99798
		Value	Standard Error
a	Intercept	148.70723	4.20896
	Slope	23200.70666	36.19036
b	Intercept	103.73521	4.39019
	Slope	24385.90761	37.74861
c	Intercept	148.70723	4.20896
	Slope	23200.70666	36.19036

Figure 28. The deformation curves PMAA-*l*-PIB-850-pH7

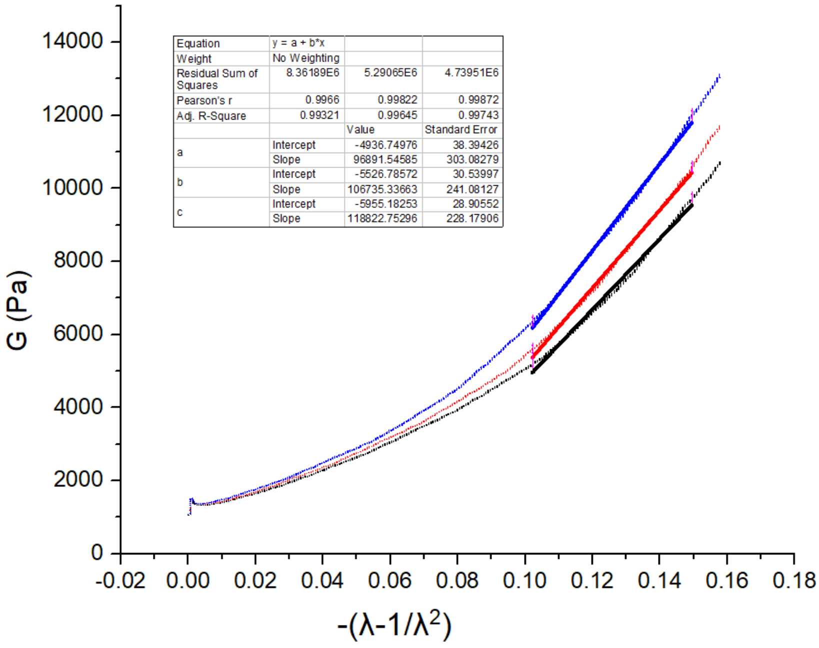

Equation	y = a + b*x		
Weight	No Weighting		
Residual Sum of Squares	8.36189E6	5.29065E6	4.73951E6
Pearson's r	0.9966	0.99822	0.99872
Adj. R-Square	0.99321	0.99645	0.99743
		Value	Standard Error
a	Intercept	-4936.74976	38.39426
	Slope	96891.54585	303.08279
b	Intercept	-5526.78572	30.53997
	Slope	106735.33663	241.08127
c	Intercept	-5955.18253	28.90552
	Slope	118822.75296	228.17906

Figure 29. The deformation curves PMAA-*l*-PIB-860-pH7

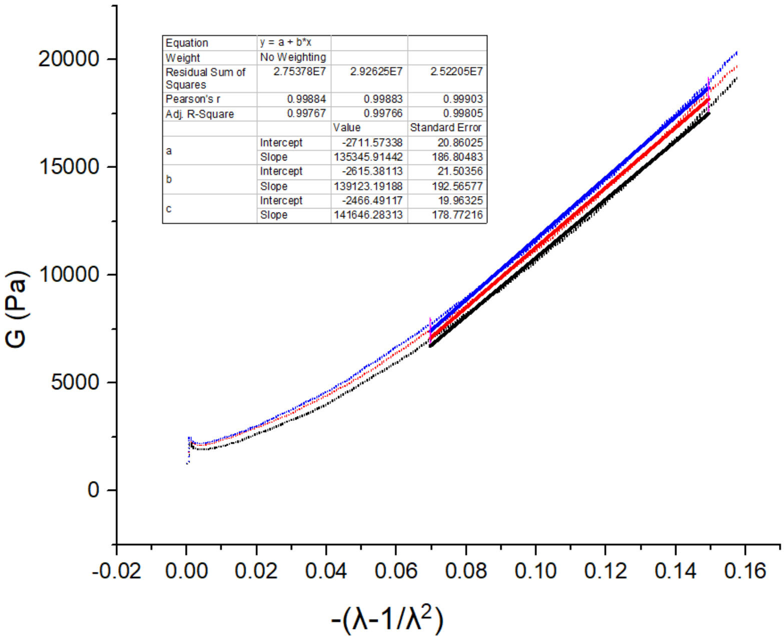

Equation	y = a + b*x		
Weight	No Weighting		
Residual Sum of Squares	2.75378E7	2.92625E7	2.52205E7
Pearson's r	0.99884	0.99883	0.99903
Adj. R-Square	0.99767	0.99766	0.99805
		Value	Standard Error
a	Intercept	-2711.57338	20.86025
	Slope	135345.91442	186.80483
b	Intercept	-2615.38113	21.50356
	Slope	139123.19188	192.56577
c	Intercept	-2466.49117	19.96325
	Slope	141646.28313	178.77216

Figure 30. The deformation curves PMAA-*l*-PIB-870-pH7

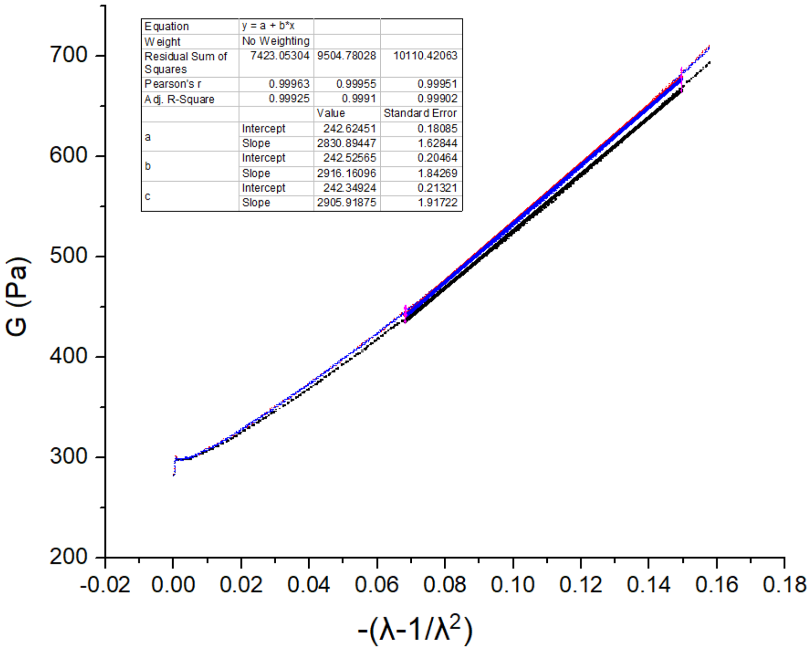

Equation	y = a + b*x		
Weight	No Weighting		
Residual Sum of Squares	7423.05304	9504.78028	10110.42063
Pearson's r	0.99963	0.99955	0.99951
Adj. R-Square	0.99925	0.9991	0.99902
		Value	Standard Error
a	Intercept	242.62451	0.18085
	Slope	2830.89447	1.62844
b	Intercept	242.52565	0.20464
	Slope	2916.16096	1.84269
c	Intercept	242.34924	0.21321
	Slope	2905.91875	1.91722

Figure 31. The deformation curves PMAA-*l*-PIB-1020-pH7

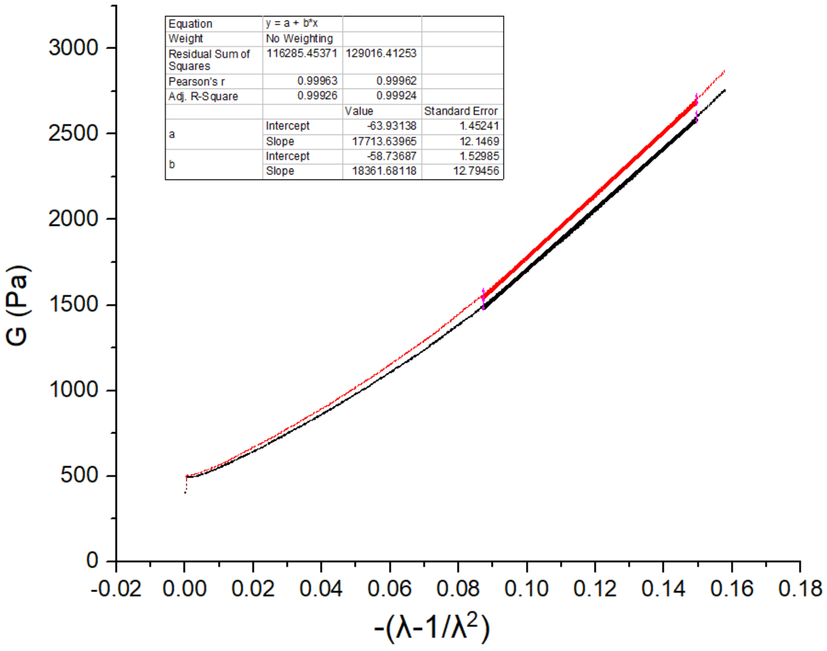

Equation	y = a + b*x		
Weight	No Weighting		
Residual Sum of Squares	116285.45371	129016.41253	
Pearson's r	0.99963	0.99962	
Adj. R-Square	0.99926	0.99924	
		Value	Standard Error
a	Intercept	-63.93138	1.45241
	Slope	17713.63965	12.1469
b	Intercept	-58.73687	1.52985
	Slope	18361.68118	12.79456

Figure 32. The deformation curves PMAA-*l*-PIB-1030-pH7

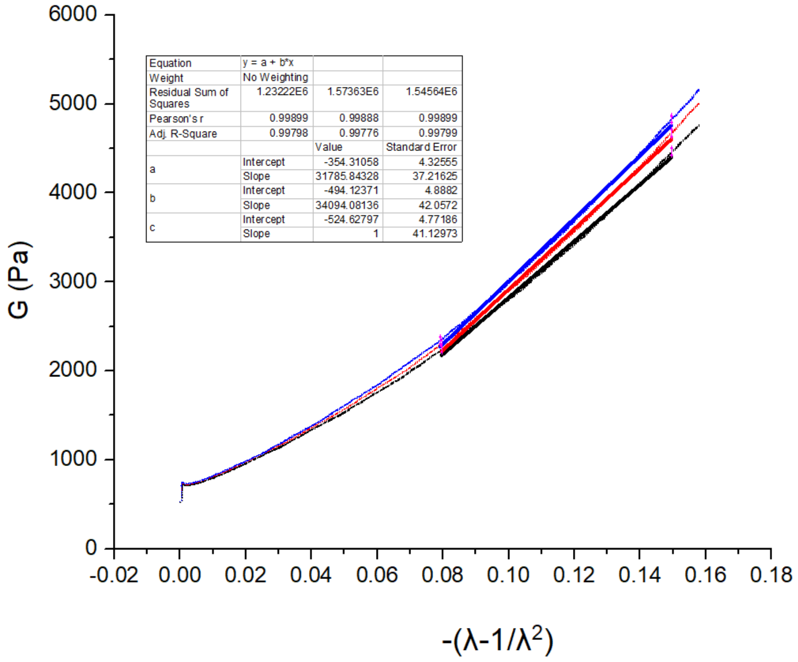

Equation	y = a + b*x		
Weight	No Weighting		
Residual Sum of Squares	1.23222E6	1.57363E6	1.54564E6
Pearson's r	0.99899	0.99888	0.99899
Adj. R-Square	0.99798	0.99776	0.99799
		Value	Standard Error
a	Intercept	-354.31058	4.32555
	Slope	31785.84328	37.21625
b	Intercept	-494.12371	4.8882
	Slope	34094.08136	42.0572
c	Intercept	-524.62797	4.77186
	Slope	1	41.12973

Figure 33. The deformation curves PMAA-*l*-PIB-1040-pH7

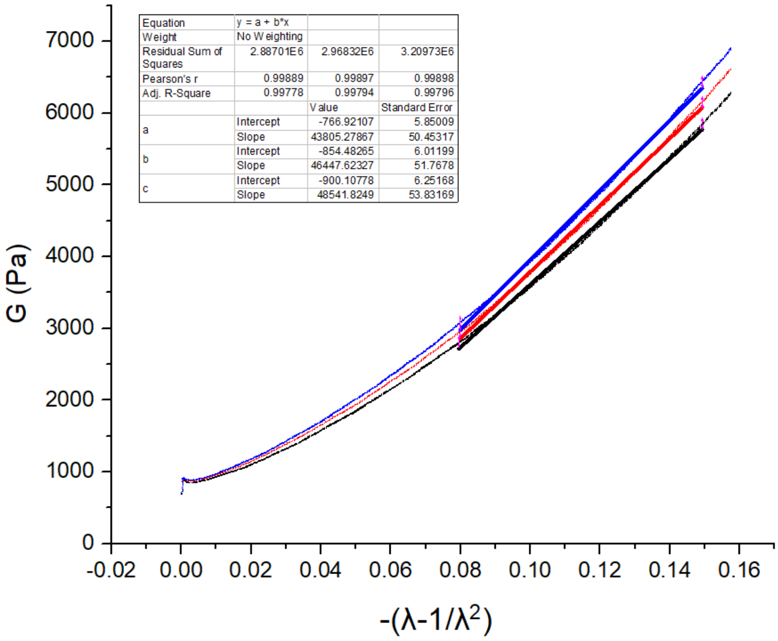

Equation	y = a + b*x		
Weight	No Weighting		
Residual Sum of Squares	2.88701E6	2.96832E6	3.20973E6
Pearson's r	0.99889	0.99897	0.99898
Adj. R-Square	0.99778	0.99794	0.99796
		Value	Standard Error
a	Intercept	-766.92107	5.85009
	Slope	43805.27867	50.45317
b	Intercept	-854.48265	6.01199
	Slope	46447.62327	51.7678
c	Intercept	-900.10778	6.25168
	Slope	48541.8249	53.83169

Figure 34. The deformation curves PMAA-*l*-PIB-1050-pH7

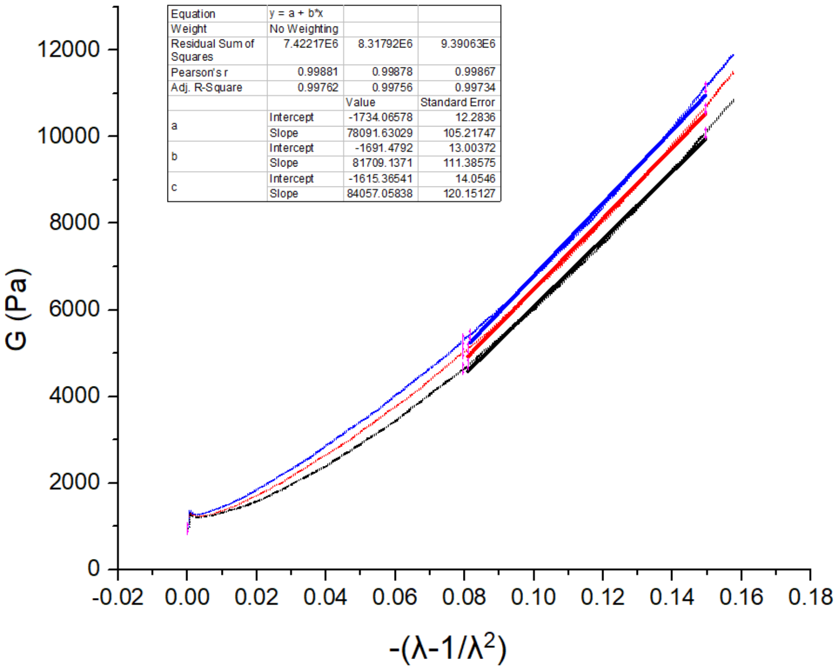

Equation	y = a + b*x		
Weight	No Weighting		
Residual Sum of Squares	7.42217E6	8.31792E6	9.39063E6
Pearson's r	0.99881	0.99878	0.99867
Adj. R-Square	0.99762	0.99756	0.99734
		Value	Standard Error
a	Intercept	-1734.06578	12.2836
	Slope	78091.63029	105.21747
b	Intercept	-1691.4792	13.00372
	Slope	81709.1371	111.38575
c	Intercept	-1615.36541	14.0546
	Slope	84057.05838	120.15127

Figure 35. The deformation curves PMAA-*l*-PIB-1060-pH7

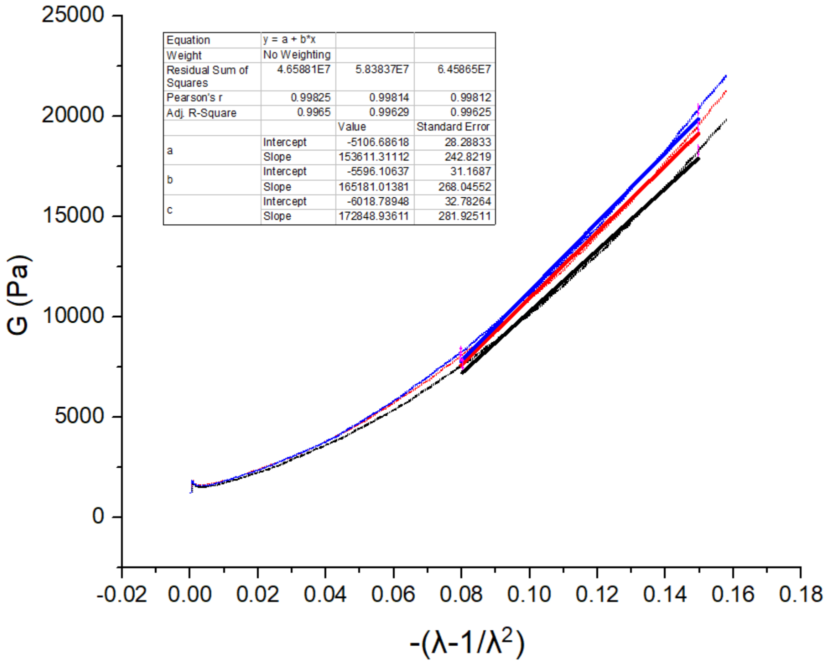

Equation	y = a + b*x		
Weight	No Weighting		
Residual Sum of Squares	4.65881E7	5.83837E7	6.45865E7
Pearson's r	0.99825	0.99814	0.99812
Adj. R-Square	0.9965	0.99629	0.99625
		Value	Standard Error
a	Intercept	-5106.68618	28.28833
	Slope	153611.31112	242.8219
b	Intercept	-5596.10637	31.1687
	Slope	165181.01381	268.04552
c	Intercept	-6018.78948	32.78264
	Slope	172848.93611	281.92511

Figure 36. The deformation curves PMAA-*l*-PIB-1070-pH7

Figyelmeztetés! A kitöltött Nyilatkozat nem menthető el, csak kinyomtatható! **Nyomtatás**

NYILATKOZAT

Név: Edwin Steven Reyes Jacome

ELTE Természettudományi Kar, szak: Materials Science MSc

NEPTUN azonosító: DHDB3B

Diplomamunka címe:
Mechanical properties of swollen poly(methacrylic acid)-l-polyisobutylene conetworks

A **diplomamunka** szerzőjeként fegyelmi felelősségem tudatában kijelentem, hogy a dolgozatom önálló szellemi alkotásom, abban a hivatkozások és idézések standard szabályait következetesen alkalmaztam, mások által írt részeket a megfelelő idézés nélkül nem használtam fel.

Budapest, 2024-01-02

a hallgató aláírása